OPTIMIZATION OF A MICROFLUIDIC CHIP DESIGN FOR NEUROBLASTOMA CELLS AND THEIR MICROENVIRONMENT STUDIES

by

Kübra GÖKMEN

B.S., in Bioengineering, Yıldız Technical University, 2013

Submitted to the Institute of Biomedical Engineering
in partial fulfillment of the requirements
for the degree of
Master of Science
in
Biomedical Engineering

Boğaziçi University
2022

ACKNOWLEDGMENTS

First of all, I would like to thank my supervisor Assoc. Prof. Dr. Özgür Kocatürk for involving me in this project and giving me the opportunity to work with him. I am grateful for his suggestions and guidance during my thesis studies.

I would like to express my sincere gratitude to my co-supervisor Prof. Dr. Numan Akdoğan for every opportunity that he provided me during my studies. This thesis would have not been completed without his guidance, knowledge, and endless support.

In addition, I am very thankful to Assoc. Prof. Dr. Bora Garipcan for giving me access to work in the cell culture laboratory.

I warmly thank Elif Dönmez to share her knowledge and for her contribution to my thesis. I am grateful for her support and friendship.

My appreciation extends to the people at Gebze Technical University. I would like to thank Dr. Şafak Gök for his guidance during my cleanroom studies at Gebze Technical University. I also would like to mention how grateful I am for meeting Dr. Hasan Pişkin and Davut Yıldırım at GTU. I owe my special thanks to them for sharing their knowledge whenever I need it and for their friendship.

I also thank Ahmet Turan Talaş and Hasan Şahin for their support during my cleanroom studies at Boğaziçi University.

And there are countless people from my BME family that I want to thank. I owe my special thanks to Fatma Zehra Erkoç, Hatice Oruçoğlu, Hayriye Oztatlı, Ecem Sakallı, Morteza Teymoori, Bengü Aktaş, Meryem Şahin Erdoğan, and Cansu Şen for their support and friendship.

Finally, I would like to express my gratitude to my dear parents and lovely sisters, to whom this thesis is dedicated, for their support in every step that I take. Feeling their presence and unconditional love in every part of my life is a priceless gift for me. I am very thankful to them for keeping me motivated, encouraging me whenever I let my guard down, and making my life easier.

ACADEMIC ETHICS AND INTEGRITY STATEMENT

I, Kübra Gökmen, hereby certify that I am aware of the Academic Ethics and Integrity Policy issued by the Council of Higher Education (YÖK) and I fully acknowledge all the consequences due to its violation by plagiarism or any other way.

Name :

Signature:

Date:

ABSTRACT

OPTIMIZATION OF A MICROFLUIDIC CHIP DESIGN FOR NEUROBLASTOMA CELLS AND THEIR MICROENVIRONMENT STUDIES

Investigating each structural part of a neuron is crucial for clarifying the complex working mechanism of the nervous system. Isolation of axons from their cell bodies plays an important role in understanding synapse formation, axonal injury and regeneration mechanisms, and the interaction between the neurons and their microenvironments. Multi-compartment microfluidic chips are one of the most developed systems used for axon isolation. In this thesis, the optimization of microfluidic chip production has been carried out by changing photoresist types and UV exposure doses, and the effects of these variables on the microgroove width have been observed. For this purpose, two-step photolithography processes have been performed using SU-8 3005, SU-8 3050 SU-8 2005, and SU-8 2050 negative photoresists. Optimum microgroove width (7.3 μm) to isolate axons has been obtained by using SU-8 3005 and applying UV exposure for 3 seconds with a power of 21 mW/cm^2. A similar microgroove width (7.7 μm) has also been achieved by using a different mask alignment system operating outside the cleanroom conditions, and it has been evaluated as promising in terms of reducing microfluidic chip manufacturing costs. SH-SY5Y neuroblastoma cells have been seeded into the microfluidic chips with different microgroove geometries (4.4×10.2 μm, 4.4×7.3 μm, and 4×7.7 μm) through filtered micropipette tips and 8 mm wide reservoirs. The second seeding method has been found more efficient in terms of applicability and sustainability. It has also been observed that 4.4×10.2 μm geometry allowed cell migration in both cell culture methods while the other two geometries provided axon isolation. In conclusion, obtained microfluidic chips and improved cell culture method has been considered suitable to investigate the neurite elongation and differentiation of SH-SY5Y cells, and their interaction with their microenvironment.

Keywords: Axon isolation, microfluidic neuron chip optimization, photolithography

ÖZET

NÖROBLASTOM HÜCRELERİ VE MİKROÇEVRE ÇALIŞMALARI İÇİN MİKROAKIŞKAN ÇİP TASARIMININ OPTİMİZASYONU

Bir nöronun her bir yapısal parçasını araştırmak, sinir sisteminin karmaşık mekanizmasını açıklamak için çok önemlidir. Aksonların hücre gövdelerinden izole edilmesi; sinaps oluşumu, aksonal hasar ve rejenerasyon mekanizmalarının ve nöronlar ile mikroçevreleri arasındaki etkileşimin anlaşılmasında önemli bir rol oynar. Çok bölmeli mikroakışkan çipler, akson izolasyonu için kullanılan en gelişmiş sistemlerden biridir. Bu tezde, fotorezist çeşitleri ve UV maruziyet dozları değiştirilerek mikroakışkan çip üretiminin optimizasyonu sağlanmış ve bu değişkenlerin mikro oluk genişliği üzerindeki etkileri incelenmiştir. Bu amaçla, SU-8 3005, SU-8 3050 SU-8 2005 ve SU-8 2050 negatif fotoresistler kullanılarak iki-adımlı fotolitografi işlemleri gerçekleştirilmiştir. Aksonları izole etmek için optimum mikro oluk genişliği (7.3 μm), SU-8 3005 kullanılarak ve 21 mW/cm^2 gücünde 3 saniye UV maruziyeti uygulanarak elde edilmiştir. Temizoda koşulları dışında çalışan farklı bir maske hizalama sistemi de kullanılarak benzer mikro oluk genişliği (7.7 μm) elde edilmiş ve mikroakışkan çip üretim maliyetini düşürmesi açısından umut verici olarak değerlendirilmiştir. SH-SY5Y nöroblastom hücreleri, filtrelenmiş mikropipet uçları ve 8 mm genişliğinde rezervuarlar aracılığıyla farklı mikro oluk geometrilerine (4.4×10.2 μm, 4.4×7.3μm ve 4×7.7 μm) sahip mikroakışkan çiplere ekilmiştir. İkinci ekim yöntemi uygulanabilirlik ve sürdürülebilirlik açısından daha verimli bulunmuştur. Her iki hücre kültürü yönteminde de 4.4×10.2 μm geometrisinin hücre göçüne izin verdiği, diğer iki geometrinin ise akson izolasyonu sağladığı görülmüştür. Sonuç olarak, optimize edilen mikroakışkan çipler ve hücre kültürü yöntemlerinin; nörit uzamasını, SH-SY5Y hücrelerinin farklılaşmasını ve mikro çevreleri ile etkileşimlerini araştırmak için uygun olduğu görülmüştür.

Anahtar Sözcükler: Akson izolasyonu, mikroakışkan nöron çip optimizasyonu, fotolitografi

TABLE OF CONTENTS

LIST OF FIGURES

LIST OF TABLES

LIST OF SYMBOLS

°C	Degree Celsius
W	Watt
mL	Mililiter
mg	Miligram
mbar	Milibar
μm	Micrometer
cm^2	Square Centimeter
μL	Microliter

LIST OF ABBREVIATIONS

ABS	Acrylonitrile Butadiene Styrene
ANS	Autonomic Nervous System
CO_2	Carbon Dioxide
CNS	Central Nervous System
CVD	Chemical Vapor Deposition
EtOH	Ethanol
FBS	Fetal Bovine Serum
FDM	Fused Deposition Modeling
GTU	Gebze Technical University
N_2	Nitrogen Gas
NGF	Neuron Growth Factor
PNS	Peripheral Nervous System
PBS	Phosphate Buffered Saline
PC	Polycarbonate
PDMS	Polydimethylsiloxane
PLA	Polylactic Acid
PLL	Poly L-lysine
proNGF	pro Nerve Growth Factor
RNA	Ribonucleic Acid
Si-OH	Silanol
SiO_2	Silicon dioxide
Si-O-Si	Siloxane Bonds
3D	Three Dimensional
UV	Ulraviolet

1. INTRODUCTION

The nervous system has a unique complex structure that coordinates all the activities in the organisms by transmitting the signals through the body to respond to and adapt to the changes [1, 2, 3]. Neurons are functional units of the nervous system which contain soma, axon, and dendrites in their structures [4, 5]. This complex system is one of the most studied areas by researchers to understand the function of neurons and their interactions with their microenvironment [3, 6]. Understanding the structure and function of each element of a neuron plays an important role in clarifying the mechanism of the nervous system [6, 7, 8, 9].

Although some basic studies can be applied in traditional cell culture methods like cell loading in a petri dish, these methods are not applicable for creating an extracellular environment or isolation of axons and cell bodies of neurons [3, 6, 10]. Therefore, these in vitro studies need to be supported by animal models to observe the in vivo physiological results such as immune response and tissue reactions [3, 11].

However, it is not possible to mimic human physiology in animal studies because human cells cannot directly be applied to animal models. Moreover, ethical issues, space and effort needed for practicing animal studies, and the high cost of the applications are some other limitations of practicing in vivo research in animal models [12, 13].

To eliminate the above-mentioned limitations for researching the nervous system, scientists have modified the traditional technologies and developed compartmentalized culture systems. These new techniques are mainly based on isolating axons from the cell body to be able to investigate axonal growth and transportation, axonal injury and regeneration [9], synapse biology, and interactions between nerve cells and other cells [6, 10, 14]. Campenot Chamber [15], Boyden Chamber [16], and Microfluidic Chips [6, 17] are the main compartmentalized culture systems that are used for

nervous system investigations. Microfluidic chips are developed by improving the first 2 techniques [6], and they allow a controllable environment with easy adaption of the system according to the study requirements [12]. Microfluidic chips provide advantageous cell culturing platforms to imitate the neuron microenvironment [8, 9, 17, 18]. Multi-compartment microfluidic chips give the opportunity to separate the axonal and somal sides of the nerve cells for investigating each part individually [9, 17, 18].

Microfluidic chips have patterned features in micron sizes and these chips mainly consist of polymers such as polydimethylsiloxane (PDMS) since it is optically transparent and biocompatible. There are many fabrication methods and materials for manufacturing microfluidic chips and those can be chosen depending on the requirements of the studies. Lithography techniques, molding methods, and 3D printing technologies are some of the techniques used for microfluidic chip production [12, 19, 20].

Advanced and interdisciplinary technologies are implemented in microfluidic chip systems for applications in different fields. They can be used in many fields such as therapy and diagnosis, cell culture studies, organ-on chips, and pharmaceutical applications. Microfluidic chip technology provides more advantages in terms of sample amount, required time, and flexible design options compared to traditional methods [12, 13].

There are many studies in the literature for the investigation of the interactions between nerve cells and different cells in their microenvironments [6, 7, 21]. But the "know-how" of these studies is clearly explained in the literature. Therefore, the main purpose of this thesis is to demonstrate the important points of microfluidic chip production to the researchers. In addition, it is aimed to optimize the fabrication of a neuron chip with reference to the previous compartmentalized microfluidic chip [6] studies to investigate nerve cells and their microenvironment. The chip model mainly consists of two separate channels which are connected through parallel microgrooves. Photoresist models SU-8 2005 and SU-8 3005 with different densities have been used to obtain the optimum microgroove size required for axonal isolation, and the efficacy of those UV light-sensitive liquid coating materials have been compared in different UV

exposure periods. SH-SY5Y neuroblastoma cells have been cultured into the chips with different microgroove sizes by using two different static culture methods to compare the effect of the culture method and microgroove size.

This thesis reported the optimum microgroove size and cell culture method for the axonal isolation of SH-SY5Y neuroblastoma cells. This optimized microfluidic neuron chip model can be used in future studies for observing SH-SY5Y neuroblastoma cell differentiation, neurite elongation, and microenvironment interaction in both static and dynamic cultural environments.

2. BACKGROUND

2.1 Nervous System

The nervous system is responsible for coordinating all activities in the body and it allows the body to respond and adapt to the changes happening inside or outside of the body. The nervous system is subdivided into two categories which are Central Nervous System (CNS) and Peripheral Nervous System (PNS) [1, 2, 22].

The CNS consists of the brain and spinal cord, and it conducts and processes signals as a control center of the body [22, 23, 24]. The CNS has an important role in the studies to understand the behavior of humans or animals. It is also related to partner selection, integration into social systems, or expression and processing of emotions [1, 24]. The PNS is classified into Somatic Nervous System (SNS) and Autonomic Nervous System (ANS). Actions occurring in the somatic nervous system are mostly conscious and subject to voluntary control [1]. Nerve fibers in the somatic nervous system extend from and to the sense organs, skin, and skeletal muscles, and they create a response to stimuli coming from the outside environment. On the other hand, most of the activities happening through the ANS are involuntary processes. This system consists of efferent neurons, and it mainly functions to regulate the internal environment of the body by managing the internal organs, circulatory system, and sexual functions [1, 2].

2.2 Anatomy and Functions of The Neurons

Neurons, the excitable cells that send and receive signals through action potentials, are the nervous system's basic functional and structural units. Neurons are structurally composed of soma, axon, and dendrites [1, 2]. Soma has an axon hillock and the axon originates from here [1]. Axon transfers efferent neural signals to neighbor

neurons and close or distant effectors. Axons generally split up into branches that end in presynaptic terminals. Dendrites transmit excitatory or inhibitory signals that they receive from other neurons to the cell body. A single neuron may have many dendrites resulting from receiving many input signals [1, 24, 25] Axolemma which is the plasma membrane of the axon is surrounded by Schwann cells in the Peripheral Nervous System while it is surrounded by oligodendrocytes in the Central Nervous System [1, 24]. Axons of some neurons are covered with myelin sheat which accelerates the transmitting of nerve impulses [1]. Neuron structure and function were summarized in Figure 2.1. below.

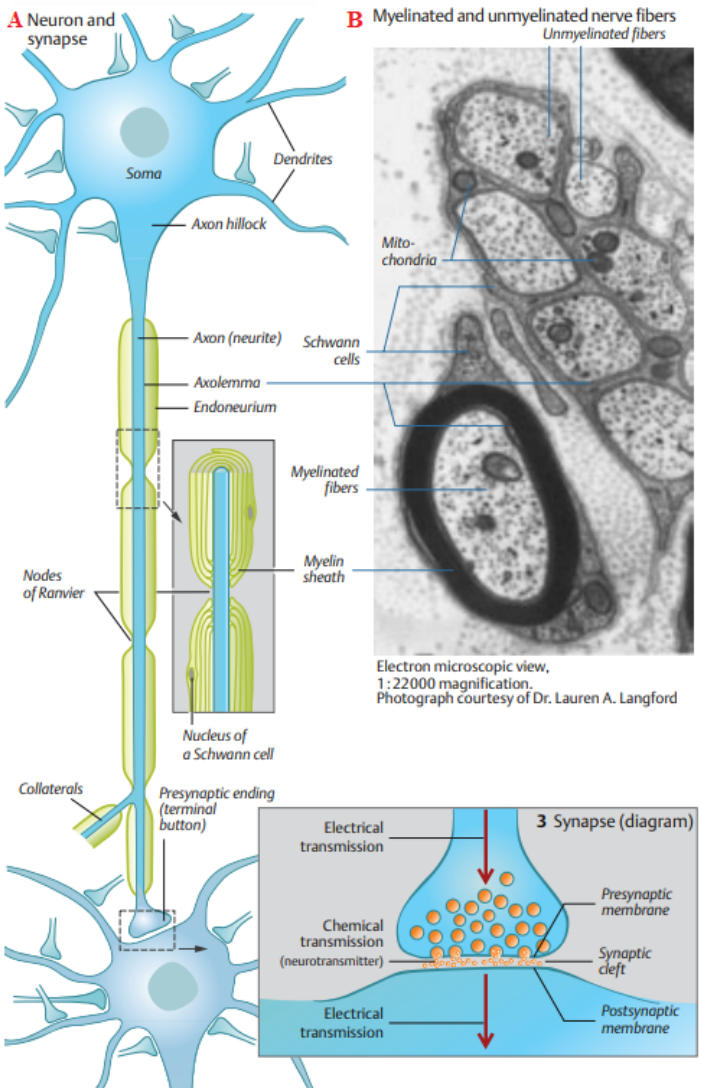

Figure 2.1 Neuron structure and function (A) Neuron structure and synapse (B) Myelinated and unmyelinated nerve fibers [1].

A synapse is the communication point of a neuron with neurons or a neuron with effectors. In this place, signals are conducted from the presynaptic membrane to the postsynaptic membrane through released neurotransmitters. Neurotransmitter molecules are bound to receptors of the postsynaptic membrane to create an inhibitory or excitatory effect [1, 2].

2.3 Axon Isolation Techniques

It has been explained in the previous part that the axons transmit neural signals through the body. They play an important role in the nervous system by connecting with other neurons and different cells which makes them crucial in synapse formation [1, 2]. Moreover, axonal damage is critically involved in CNS injuries and neurodegenerative diseases [9] In addition, it is critical to clarify the nervous system controlling mechanism in homeostatic and pathological conditions by investigating the communication between nerve cells and other cell types [6]. Therefore, some axonal isolation methods have been developed to study the human nervous system and clarify its working mechanism [6, 7].

2.3.1 Campenot Chamber

Campenot Chamber was designed by Robert Campenot to separate neuron cell bodies from axons to investigate axonal biology [6, 15]. A compartmented Teflon divider is attached to a glass coverslip or a cell culture dish via silicon grease. A cell culture dish is generally coated with collagen and parallel lines 200 μm apart are created by scratching the surface of the dish [15]. The original chip consists of 3 connected chambers which are one central compartment and two side compartments [10, 14]. Neurons are seeded in the central compartment of the Campenot Chamber, and neurite elongation through the grease layer to the adjacent compartments is generally provided with the help of the Neuron Growth Factor(NGF) [9, 10, 26]. Formation of the synapse, neuronal survival, target-derived neurotrophin-initiated signaling, and retrograde sig-

naling are some of the main studies applied in the Champenot Chamber. Although the design of the chip is good for fluidic separation, an unstable grease seal tends to create leaks between the chambers and it might cause the pass of more axons and contamination with somas [10]. The other limitation of this chip is the studied neuron type. Because of technical reasons, generally, longer axons are needed to use in the chambers which are promoted with NGF. Since the response of cerebral neurons to the NGF is different, the studies in these chips have been limited to the neurons of the peripheral nervous system [26, 27].

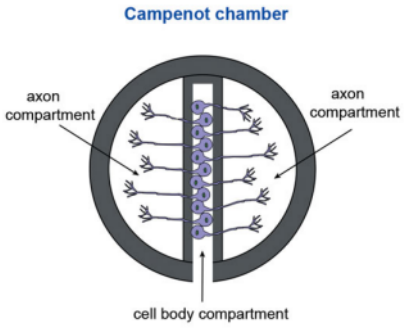

Figure 2.2 Campenot Chamber [10].

2.3.2 Modified Boyden Chamber

Boyden chamber was designed by Stephen Boyden for investigating leukocyte migration [16]. This design was then modified to segregate axons from their cell bodies by changing the pore size of the membrane which separates the compartments [28]. Boyden Chamber consists of two compartments separated by a porous membrane including pores of various sizes that acts as a physical barrier. This porous structure allows the migration of motile cells into the distal part. Neurons are seeded on the upper compartment of the chip and extended axons pass through the membrane into the lower chamber in several days [10, 14].

The simple neuronal culture process and the use of tissue explant without the need for modification are the main advantages of this method. In addition to that, collecting axonal samples easily is the other benefit of the chip. On the other hand,

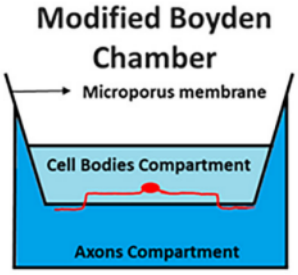

Figure 2.3 Modified Boyden Chamber [28].

there is a limitation while studying axon-specific stimulation. Since the fluidic separation between chambers is not possible, cell bodies are required to be removed. Another disadvantage of the system is having difficulties in getting clear images and limiting the morphological studies due to the axons grown on the porous membrane [10, 14].

2.3.3 Microfluidic Chips

Designing microfluidic chips for studying neurobiology is developed by modifying the original idea of the Campenot Chamber. Microfluidic chips have offered a broad range of study areas in neuroscience by eliminating the restrictions of the Campenot Chamber which are axonal isolation problems and limited nerve cell type that can be studied in it [6].

The application of microfluidic technology for neurobiological studies was first used by Anne M. Taylor [29]. This two-compartment microfluidic chip was designed to allow fluidic separation of cell bodies from axons. In this design, neurons can be plated in one compartment of the microfabricated neuronal culture chip and let axons grow through the microgrooves to reach the adjacent compartment. Polydimethylsiloxane (PDMS) which is a biologically inert and transparent material is used for the fabrication of compartmentalized microfluidic chips for neuron studies. Accurately patterned features are obtained by the photolithography method to use as a mold for PDMS casting. The chip obtained from PDMS consists of two main channels 100 μm high,

1.5 mm wide, and 8 mm long which are connected by microgrooves 3 μm high and 10 μm wide [6, 9, 29]. The fabrication method of this chip is summarized in Figure 2.4. below. A detailed explanation of the fabrication techniques will be explained in Section 2.4.

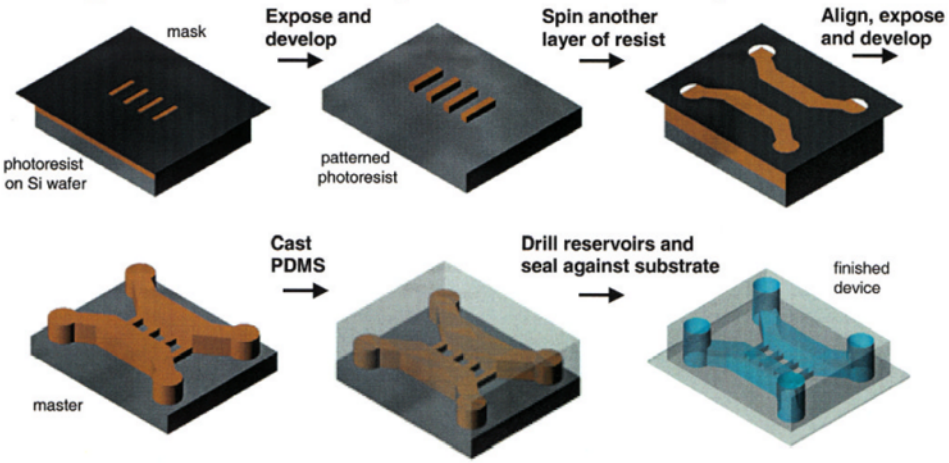

Figure 2.4 Fabrication process of microfluidic neuron chip [29].

This simple chip design has been used by many other researchers as a reference and has been improved and modified for further studies. Developed microfluidic chips have been used for researching axonal behaviors for decades. Axonal degeneration, development of in vitro disease models, drug screening, understanding the synapse function, and isolation of micro RNAs are some of the studies that have been applied to microfluidic neuron chips.

In addition, these multicompartment chips allow for studying cocultures. Despite most of the coculture studies being based on intra-system cocultures such as coculture of neurons and oligodendrocytes or neurons and Schwann cells, intersystem coculture studies have also been carried out in these systems. Observing the interactions between neurons and bone cells, muscle cells, or cancer cells some of the studies have been made via microfluidic neuron chips [6]. One of the good examples of intersystem coculture studies has been applied to investigate the interactions between cancer cells and neurons in 2016. The traditional microfluidic chip was used to understand

the cross-talk between different cancer cells and neurons. In conclusion, cancer cell migration was observed [6, 7] as demonstrated in Figure 2.5 B below.

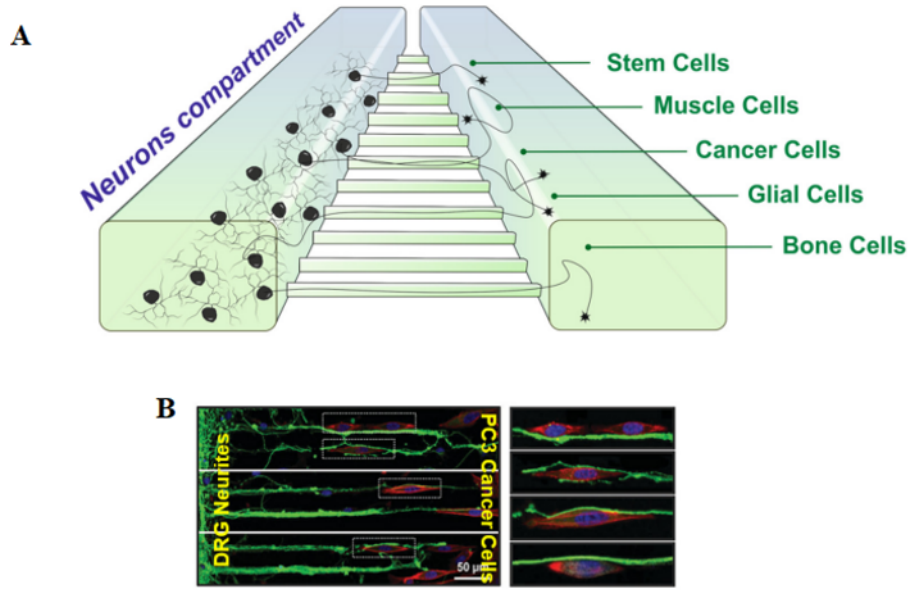

Figure 2.5 (A) Coculture systems in a compartmentalized microfluidic chip (B) Coculture of DRG neurons (green) and cancer cells (red) (modified from [6]).

Another example of co-culture studies was applied in a modified compartmentalized chip to investigate the communications between CNS neurons and glial cells, axonal specific responses and differentiation, and the development of oligodendrocytes. Thanks to the special design of this chip six different pharmacological treatments were applied to observe the effects in a single chip. The detailed shape of the chip was demonstrated in Figure 2.6. below. As a result of the study, it was demonstrated that astrocytes induced the development of oligodendrocytes, and it was observed that mature oligodendrocytes are needed for obtaining a strong myelin sheath [21, 30].

A different chip was designed by modifying one of the first multicompartment chips developed by Park et al. (2016) by creating a novel 3-compartment microfluidic chip to investigate in vitro synaptic competition. In this study, it was observed that axons in the central compartment, which were grown through the untreated neurons, created more synapses compared to the axons derived from the chamber with inhibited neuronal culture. It has been demonstrated that axon elongation and synapse forma-

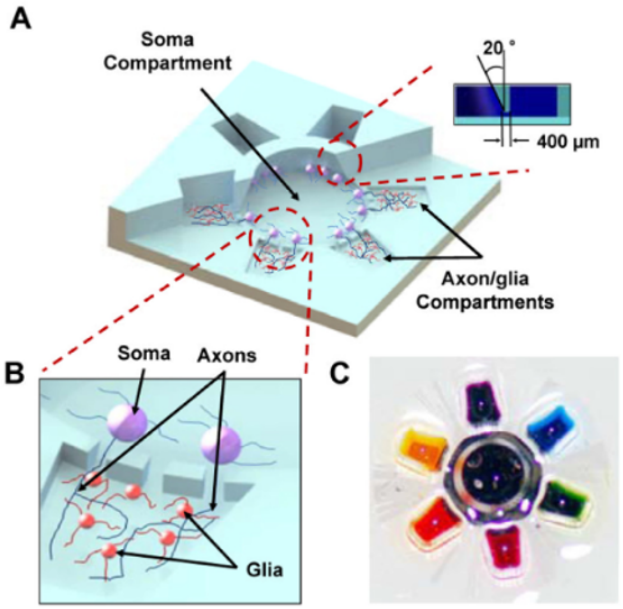

Figure 2.6 (A) 3D graphic of a neuron-glia co-culture multi-compartment system (B) Axon-glia interaction with isolated axons (C) Digital image of the system [30].

tion can be affected by decreasing neuronal activity [6, 31]. The design of the chip was shown in Figure 2.7 below.

One of the main advantages of microfluidic chips is providing fluidic isolation between compartments by adjusting the volume of the culture medium in each chamber which creates negative hydrostatic pressure in the microgrooves [9]. Another advantage is using PDMS-based chips provides optical transparency for cell visualization, and allows controlled fluid exchange and gas permeation [6, 9, 25]. In addition, these chips are quite flexible in terms of design which can be modified depending on the cell type and process. Since microgroove length can be produced shorter than the Campenot Chamber, neurons extending shorter axons can be studied in these chips [9, 28].

On the other hand, fabrication and application techniques are more expensive than classical methods and require more experience. Evaporation is another problem while working with microscale volumes and it changes culture medium osmolarity which may result in cell death if it is not checked regularly. Shear stress is produced through laminar flow and is an important variable that can affect sensitive neurons [5, 9].

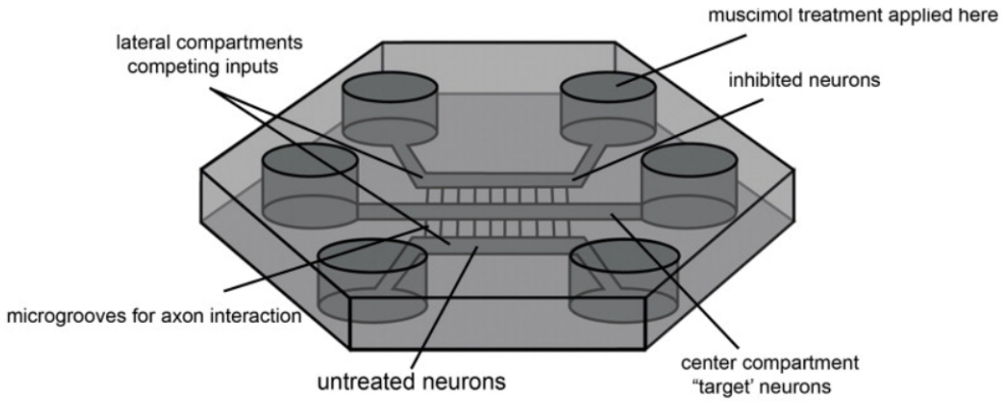

Figure 2.7 Three-compartment microfluidic chip for investigation of synapse formation [31].

2.4 Microfluidic Chip Fabrication Techniques

There are a lot of fabrication techniques to produce microfluidic chips depending on the function of use. Fabrication cost, available types of equipment, required channel size and geometry, fabrication time, and reproducibility are some of the important factors while determining the fabrication technique. In this part of the thesis, some of the popular fabrication techniques including polymer molding methods, 3D printing technologies, and UV photolithography techniques have been explained. Photolithography and soft lithography techniques have been described in more detail since those were the techniques used in the experimental method of this thesis [12, 19].

2.4.1 Photolithography

Lithography is the general name of the technique of creating patterns on a surface [32]. Photolithography is one of the most popular fabrication methods for obtaining microscale topographies. This technique is used to produce the master molds. In this process, a substrate which can be a silicon wafer or a glass, coated with the photoresist material is exposed to UV light with 365 nm or 405 nm wavelength through a predesigned photomask containing the desired patterns on it [33, 34].

Preparing the photomasks is the starting point for photolithography applications. High-resolution transparencies or chrome masks can be used as a photomask. While the patterns generally larger than 8 μm can be obtained through transparency photomasks, chrome masks allow having smaller feature sizes [19]. Chrome photomasks can be produced through laser writing devices that use a direct lithography technique. Even though this technique is expensive and time-consuming, it is preferred to obtain accurate and smaller microstructures on the masks [35]. In figure 2.8 A below, Heidelberg DWL 66fs Direct Writing Lithography Device in the cleanroom of Gebze Technical University was shown which can be used for printing the chrome photo mask.

Other components required for photolithography are a light source for UV exposure and photoresist material to transfer the designed patterns on a substrate as a result of chemical reaction [36]. SUSS-MJB4 mask aligner system in the cleanroom of Gebze Technical University was demonstrated in Figure 2.8 B. After mask preparation, the substrate is cleaned and coated with a photosensitive material, which is called photoresist, by spin coating. The coated substrate is soft-baked to densify the photoresist by evaporating the solvent from the resist and provide better adhesion to the substrate surface. Then it is exposed to UV light to transfer the patterns on the photomask to the substrate. UV light results in a chemical change in the areas that are exposed to UV light. This change is different depending on the photosensitivity of the photoresist material. There are two types of photoresists which are positive photoresists and negative photoresists. Negative photoresists harden after exposure to UV light, while UV light produces an opposite effect on positive photoresists.

After UV exposure, different steps are followed depending on the photoresist. In case of using a negative photoresist, there should be a post-exposure bake step to complete the photoreaction initiated during exposure. On the other hand, the development step can be directly followed after UV exposure when a positive photoresist is used. The developing stage is used to remove some of the photoresists in a special solution. When substrates coated with negative photoresist are immersed in the developer, parts not exposed to UV dissolve. Conversely, because of becoming soluble after UV exposure, UV-exposed areas of positive photoresist can be removed easily. Photoresist

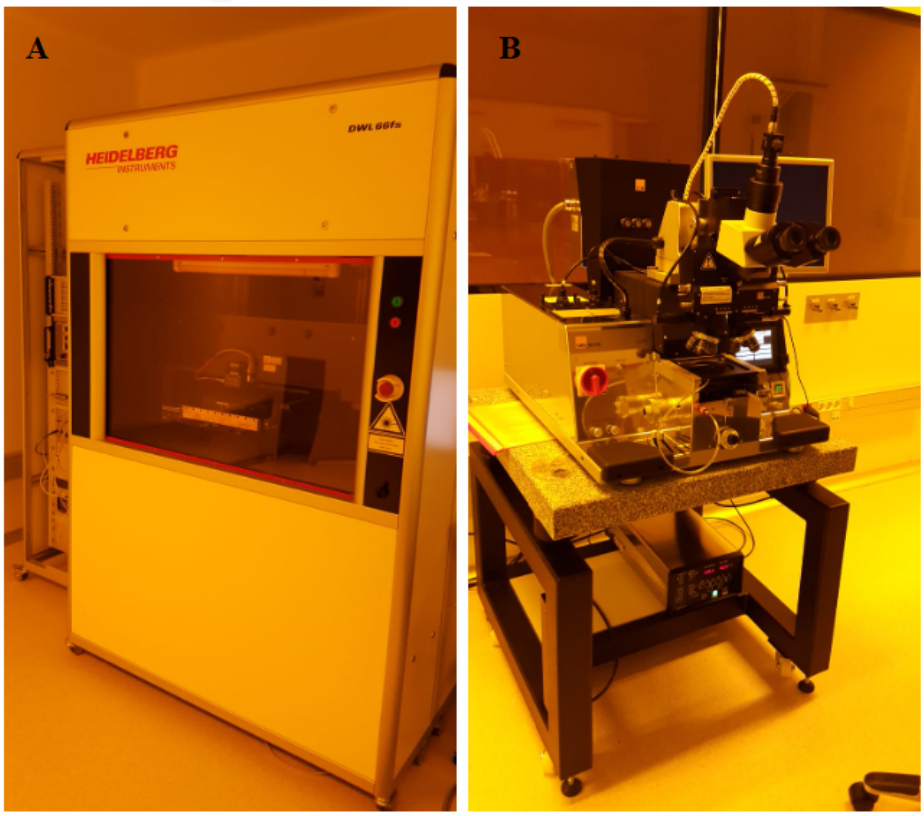

Figure 2.8 (A) Heidelberg DWL 66fs Direct Writing Lithography Device (B) SUSS-MJB4 Mask Aligner System.

types and their viscosity are important to determine the spin coating protocols, UV exposure period, and development time. These variables play an important role in determining the thickness of the microstructures [36, 37, 38, 39, 40]. The general steps of the photolithography process are summarized in Figure 2.9 below [37].

2.4.1.1 SU-8 Permanent Negative Epoxy Photoresist. SU-8 is a thermosetting polymer, that is epoxy-based and near-ultraviolet radiation sensitive, and it is one of the most preferred materials for the fabrication of microfluidic chips. Since they are thermosets, they cross-link to form rigid structures when they are exposed to heat or radiation. Once cured, it is not possible to reshape them [41, 42]. This negative photoresist has suitable mechanical and chemical features to be used in producing thick structures up to 1,5 mm high in a photolithographic single step. It is possible to produce very high aspect ratio (25:1) structures with SU-8 photoresists [42, 43, 44, 45].

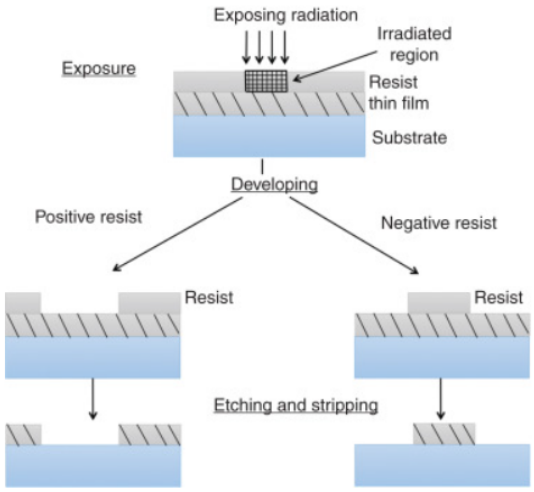

Figure 2.9 Photolithography application steps with different photoresist types [37].

SU-8 photoresists provide many advantages thanks to their high strength and stiffness, transparency, and solvent resistance in microfluidic applications [41] On the other hand, challenges in the processing steps make the repeatability of the master molds difficult. The homogeneous coating is one of the most important steps because edge bed formation during coating causes thickness variations on the substrate surface. The same problem might happen during the soft baking of photoresists. Non-uniform exposure is the other critical problem that affects reproducibility. Above mentioned problems can lead to lift-off of the whole SU-8 pattern, feature degradation, and crack-like distortions [42].

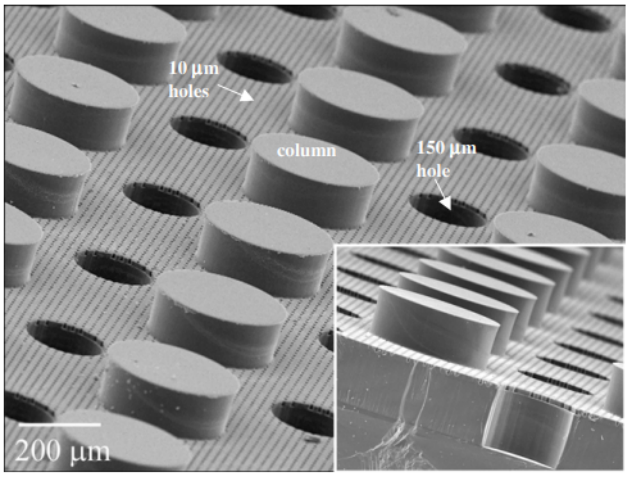

Figure 2.10 SEM image of a three-level SU-8 microstructure [42].

2.4.2 Soft Lithography

Soft lithography also known as the casting process is one of the most preferred fabrication techniques used in microfluidic chip production. In this technique, elastomeric materials are used as a stamp for creating the microstructures or to have a mold of containing the microstructures. Soft lithography is divided into different subunits such as replica molding, micro-transfer molding, microcontact printing, and solvent-assisted micro molding. In this thesis, the replica molding technique was preferred because it is the most suitable method for our needs [12, 38].

The replica molding method is applied after the photolithography process in which master mold production occurs. Polydimethylsiloxane (PDMS) is generally preferred as a silicon-based elastomer to create a replica mold. As a first step, PDMS liquid polymer is prepared by mixing the curing agent and base elastomer. Degassing of the mixture is suggested to remove the bubbles which can affect the microstructures. It is followed by pouring silicon-based elastomer onto the master mold and the curing process by heat for a certain time. As the last step, PDMS is peeled off from the master mold [19, 38]. For producing the final microfluidic chip, a PDMS replica can be reversibly sealed to different materials or irreversible bonding of PDMS with a glass or another PDMS piece can be provided by plasma cleaning [19, 37].

Soft lithography provides the advantage to obtain high-resolution replicas and complex three-dimensional structures. Another advantage of soft lithography is that it is a soft and low-cost process [19, 46].

On the other hand, the molds may deform as they are used, or even if the molds are intact, defects may occur during removing the PDMS molds from the master mold [46]. Fabrication steps of master mold production with SU-8 photoresist through photolithography and PDMS chip fabrication via soft lithography are demonstrated in Figure 2.11 below.

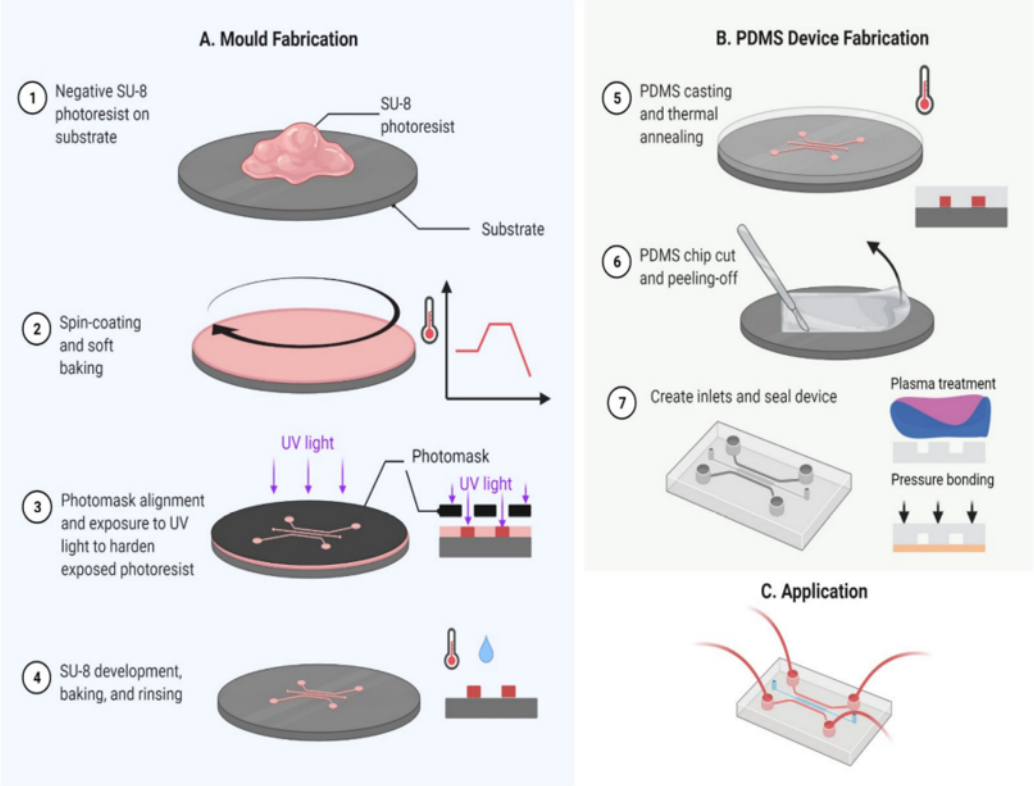

Figure 2.11 (A) SU-8 master mold fabrication (B) Soft Lithography of PDMS (C) Integration PDMS microfluidic chip with tubing [4].

2.4.2.1 Polydimethylsiloxane (PDMS). PDMS is a polymer in the class of silicone elastomers and its elasticity and biocompatibility offer a broad range of applications in the biomedical field [47, 48, 49]. PDMS contains repeated silicon and oxygen bonds and methyl groups in its chemical structure. The structure of PDMS can be modified for different applications if the methyl groups are substituted by other groups which allow for bonding between organic and inorganic groups [48, 50]. The good microstructural characteristics of PDMS material results in having good manufacturing ability by decreasing the cost. It has been proven that PDMS offers better features in microfluidic applications compared to materials like glass and silicon which were preferred in the old techniques [51, 52]. Thanks to its nontoxic, biocompatible structure with good gas permeability properties, it provides a good environment for long-term cell culture studies, screening of cells, and biochemical tests [53, 54]. Its optical transparency provides another advantage in cell culture studies for the visualization of cells [12, 55].

Even though having many advantages, PDMS has some drawbacks. Some of the advantages might also turn into disadvantages and lead to some problems during biological microfluidic applications [38]. Having a hydrophobic surface because of the methyl groups is one of the main disadvantages of PDMS for biomedical applications [48, 56]. This feature causes a problem when wetting the surface with aqueous solvents. In microfluidic applications, it can create air bubbles in the microchannels easily and leads to the absorption of hydrophobic solvents from the microchannels [19, 48, 57]. While the gas permeability of PDMS is an advantage for cell culture experiments, this porous structure can lead to some molecules diffusing into the structure. PDMS is incompatible with nonpolar, organic solvents and it swells through the adsorption of molecules of these solvents into the microchannel walls in microfluidic chips. It causes a problem in maintaining the sizes of patterned structures. In addition to that, water evaporation through the porous structure can result in a change in the solution concentration [12, 54, 55]. Another issue is thermal expansion and the softness of PDMS can cause collapsing of microstructures [38]. Although it has some drawbacks, PDMS is still preferred and widely used in biomedical applications because of its useful characteristics [38, 48].

2.4.2.2 Plasma Surface Treatment. Plasma treatment is a method used for cleaning and activating the surfaces of solid materials. Oxygen is the most used gas in the plasma treatment but nitrogen, argon, chlorine, and hydrogen bromide can also be used in this technique. Organic compounds react with the activated oxygen and form volatile products that are moved through a gas flow [58, 59, 60]. It is generally used for the activation of PDMS surfaces in microfluidic applications. PDMS has a hydrophobic surface due to the repeating -$OSi(CH_3)_2$- groups in its chemical structure. When PDMS is exposed to air or oxygen plasma, hydrocarbon groups are removed and polar silanol (Si-OH) groups are introduced so that the hydrophobic surface of PDMS is converted to a hydrophilic surface [57, 58, 60, 61]. These silanol groups on the PDMS surface can create siloxane bonds (Si-O-Si) with another activated surface that has similar silanol groups [60]. The activated surface of PDMS can regain its hydrophobic property in a short time due to the decreased surface energy when it contacts air [64].

Therefore, PDMS should be bonded either with another activated PDMS or activated glass right after plasma treatment for microfluidic chip production [60, 62]. Pressure, exposure time, and plasma power are the variables that should be optimized for an effective bonding [60]. The changes on the PDMS surface with the help of plasma treatment are demonstrated in figure 2.12.

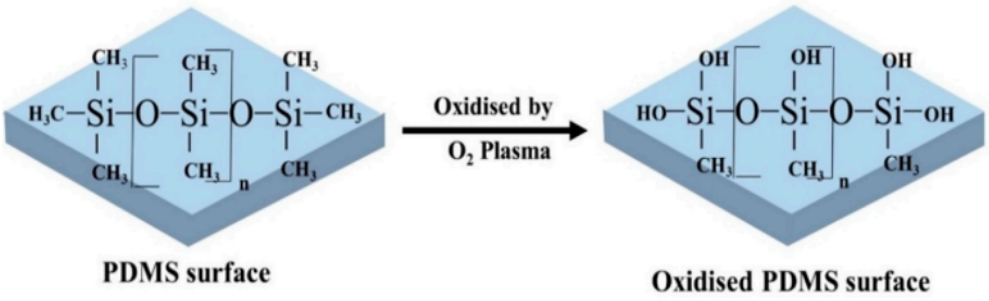

Figure 2.12 Surface modification of PDMS after oxygen plasma treatment [58].

2.4.3 Hot Embosing

The hot embossing method is used for transferring the patterns on the master mold to thermoplastic materials using heat and pressure. Thermoplastics that are used in the hot embossing process are polycarbonate, polymethylmethacrylate, cyclic olefin copolymer, and polyethylene terephthalate glycol, polystyrene, and polyvinyl chloride. This technique takes advantage of the ability of thermoplastics to be reshaped near their glass transition temperatures [19, 63, 64]. Silicon or metal materials are generally used for the fabrication of master molds. The micromachining technique can be applied to silicon wafers to obtain the silicon stamp.

On the other hand, metal master molds can be obtained by electroplating them against micromachined silicon masters [19]. Polymers are used in the film form in this technique. After the preparation of the master mold, the polymer film and master mold are heated to the glass transition temperature of the selected thermoplastic material, and the softened polymer is reshaped by applying contact pressure with the master

mold. It is followed by a cooling process of all parts and the demolding of the polymer [38]. In conclusion, a polymer containing a reversed image of the patterns on the master is obtained. The processing steps of the hot embossing technique are demonstrated in Figure 2.13 below [65].

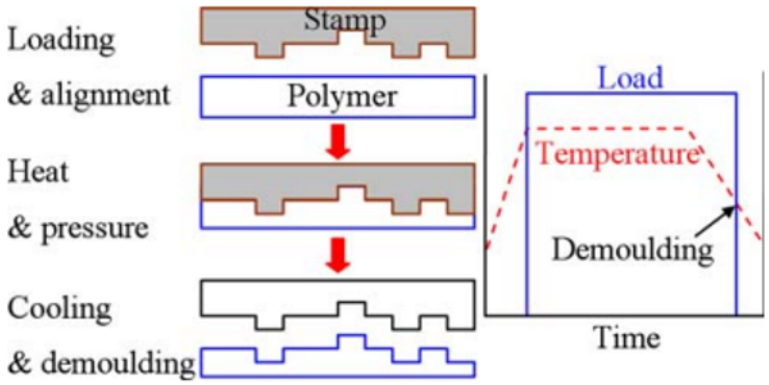

Figure 2.13 Processing steps of hot embossing technique [65].

One of the advantages of the hot embossing method is that it requires less pressure, lower flow rate, and cooling rate of polymer than used in the injection molding technique. This can result in lower internal stress and a higher aspect ratio in the final product. However, longer heating and cooling period for both polymer and mold is required compared to the injection molding technique. The whole process can take 4 to 15 minutes and sometimes it might reach 30 minutes. Some factors affect the processing steps and final product. For instance; to prevent cavity formation in the embossed polymer as a result of air trapped in the master mold, a vacuum environment is required. Temperature differences across the mold might result in bending of the produced part because of internal stress. High friction can damage the master mold and fabricated microstructures on the polymer during demolding. Having a non-sticking and smooth surface of the mold and polymer can create a solution for this problem [38].

2.4.4 Injection Molding

Injection molding is the technique commonly used to produce everyday objects by processing polymers [12, 19]. Its high throughput and precision during production and cost efficiency make this method preferable and attractive for the microfluidic chip fabrication field [12, 46].

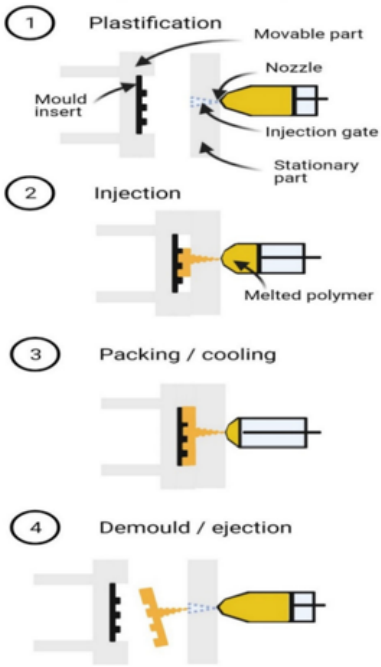

Figure 2.14 Injection molding steps[38].

It is generally known as micro-injection molding and thermoplastics are used for processing. In the first step, prepolimerized thermoplastic pellets such as PMMA are melted to a liquid state and injected into the mold cavity under high pressure [12, 19, 38, 46]. Then the temperature is decreased below the glass transition temperature of the polymer and it is cooled to have a solidified material for the demolding process [66, 67].

The steps of injection molding are summarized in the Figure 2.14 above. There are different materials and techniques for the production of the molds and the required production life of the mold plays an important role before choosing them. While silicon-based materials are preferred for short-term production, metals are used for creating

molds which are useful for long-term production. Resolution is dependent on the mold production method. For instance; whilst electron beam lithography holds the potential of creating a sub-micron resolution, the achieved resolution level is generally around 25 μm in the method of milling metals [46, 68]. Repeatability and lower process cycle time which can finish in a few seconds for each mold are some of the advantages of large volume productions. On the other hand, because of the fabrication costs of molds and the need of using complex equipment make it preferable for industrial production [19, 46].

2.4.5 3D Printing Technologies

Three-dimensional (3D) printing is another technique that is implemented for microfluidic channel formation. Different microfluidic chip designs can be created through this technology [55, 69, 70]. The general approach to this technology is using an additive manufacturing method. The 3D digital model is designed and 3D object is created by adding a new layer of material on top of the previous layer with the help of a 3D printer.

There are different 3D printing technologies and some of the most common methods have been explained briefly in this chapter [12, 38, 46]. The fundamental difference among those technologies is the method of processing the polymers while producing the layers. While polymer is softened in some technologies, the liquid materials are cured with different techniques in others [12].

One of the most commonly used 3D printing technology is fused deposition modeling (FDM) which is based on the extrusion method. In this technology, a thermoplastic filament is melted and it is extruded through a nozzle onto a surface where it is cooled below its thermoplastic temperature for solidification. Different polymers such as acrylonitrile butadiene styrene (ABS), polycarbonate (PC), and polylactic acid (PLA) can be used in this technique [71, 72]. FDM is an affordable, simple, and rapid method for material printing but it has some limitations. It might cause shape de-

formation and leakage if printing parameters are not arranged precisely according to the thermoplastic polymer [71, 73]. Figure 2.15 demonstrates the presentation of dual-headed fused deposition modeling 3D printer [71].

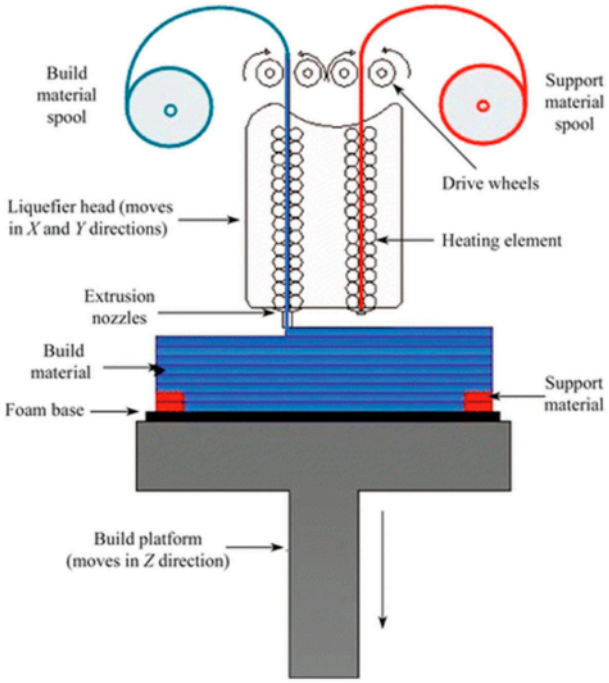

Figure 2.15 Representation of dual-headed fused deposition modeling 3D printer.

Another 3D printing technology is multi-jet modeling in which photosensitive material is used for printing. The photosensitive resin is ejected as a droplet from the printhead and cured by a light source. Above mentioned techniques are limited to print products with microscale resolutions. On the other hand, 3D printers using two-photon polymerization technology provide an advantage for producing nanometer-sized structures. Two light sources are required for this technology and it is more expensive compared to others [46].

Apart from the advantages of 3D printing technologies, there are some challenges in the fabrication of microfluidic chips. Having a microchannel size of less than 100 μm is difficult to achieve with standard 3D printing techniques. Even though microchannels having less than 100 μm in width and height is possible to produce through 3D printing, removal of the support material might damage the printed patterns [46, 74].

3. MATERIALS AND METHODS

The main purpose of this thesis is to optimize a microfluidic chip design and fabrication for providing axon isolation which can be used for investigating the interaction between nerve cells and their microenvironment in future studies. The overall chip design was created by modifying the designs used in the previous studies [6, 75] and the optimum chip was obtained by changing photoresist models and exposure dose during UV photolithography. According to the design, 5 μm width microgrooves were inserted between two main cell channels to isolate the axons from their cell bodies. SH-SY5Y neuroblastoma cells were loaded to one channel and their movement through the microgrooves was observed to determine the ideal microgroove size, and 2 different cell loading techniques were applied to observe the effects on cell movement and ease of application. A schematic representation of the microfluidic chip design according to the values included in the photomask design has been demonstrated in Figure 3.1 below.

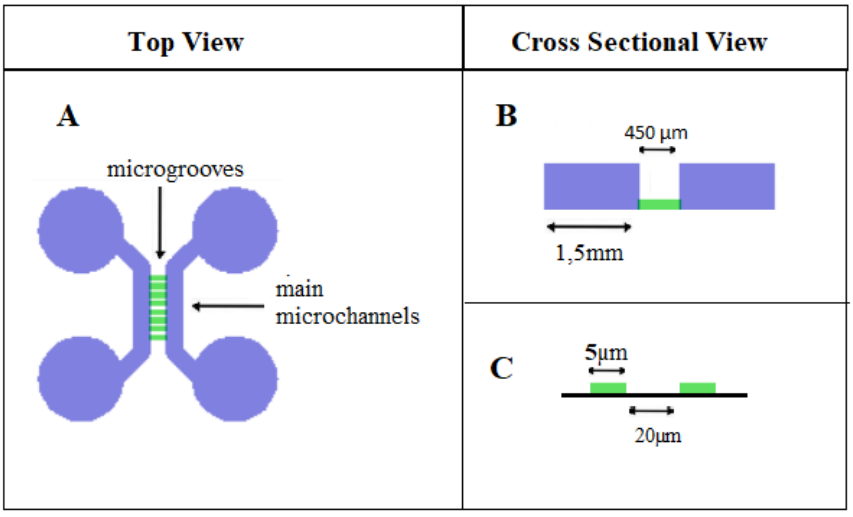

Figure 3.1 Schematic representation of the chip design (A) Top view (B) Cross sectional view of the chip showing the length of main channels (1,5 mm) and microgrooves (450 μm) (C) Cross sectional view showing the width of microgrooves (5 μm) and distance between each microgroove (20 μm).

Experimental steps followed during the microfluidic chip design and fabrication, and the cell culture studies were summarized in Figure 3.2 below.

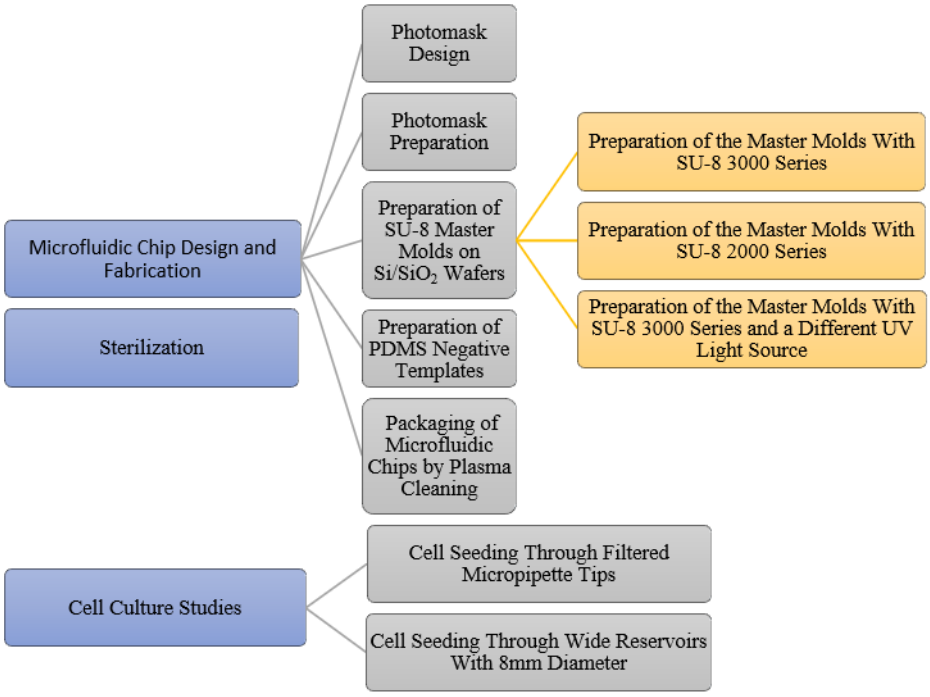

Figure 3.2 Flow chart of the experimental steps.

3.1 Microfluidic Chip Design and Fabrication

Photomask design and its preparation are initial steps to produce master molds through the UV photolithography technique. In this part of the thesis, photomask design and preparation steps were explained. This was followed by the preparation of master molds and PDMS negative templates.

3.1.1 Photomask Design

Patterns required for microfluidic chip production were designed by using CleWin 5 software (WieWeb software, Netherlands). The design was placed in a circular area with a diameter of 4 inches and divided into 3 sections for use in different photolithography applications as shown in Figure 3.3 below. While the 1st section was designed for a single-layer photolithography method, the 2nd and the 3rd sections were designed to form the layers of the two-step photolithography.

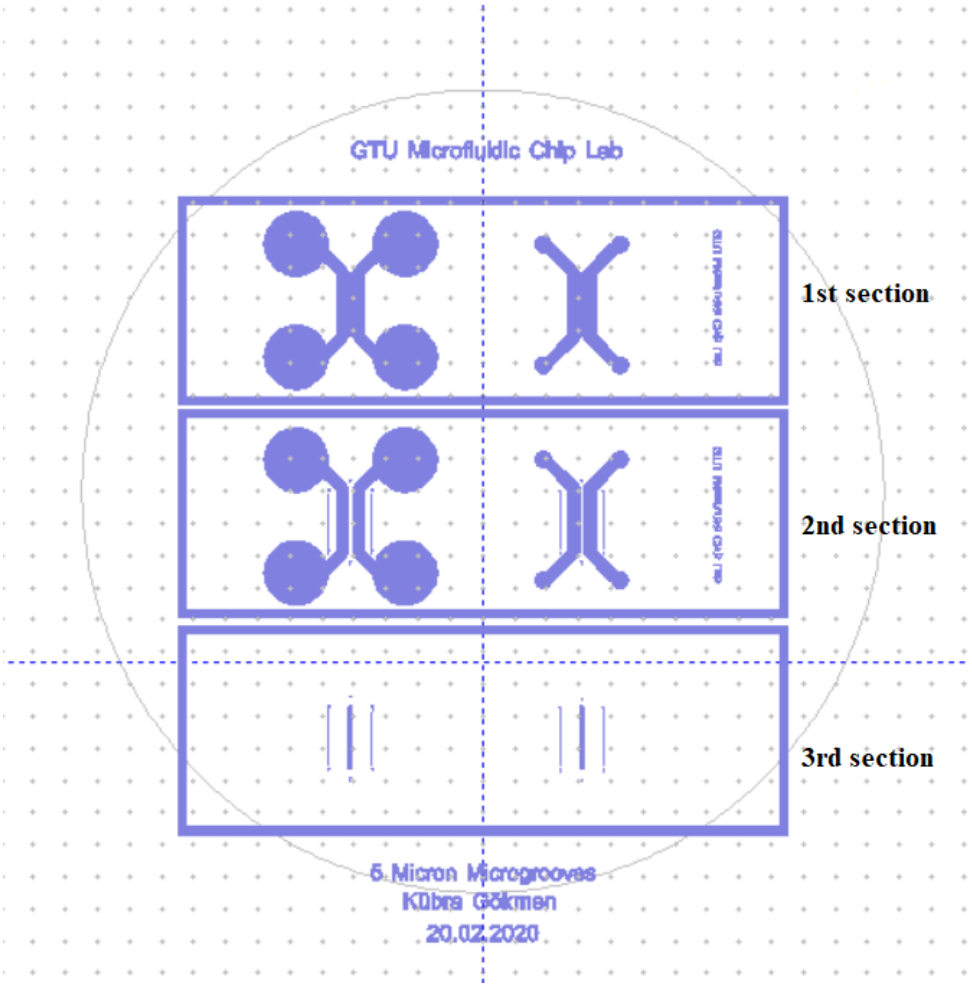

Figure 3.3 A representative image of the 5 inch mask design.

Each microfluidic chip design consists of 2 different cell channels which are in the size of 1.5 mm wide and 8 mm long. The main channels are connected to each other by microgrooves 5 μm wide and 400 μm long. There are 320 microgrooves between the main channels and the space between each microgroove is 20 μm. There are support structures extending vertically with a width of 50 μm on both sides of the microchannels for easy alignment. 25 μm from each side of these structures will be covered by the main channels and the total microgroove length will be 450 μm. Those microgrooves were designed to prevent the cell migration to the other channel and to observe the neurite elongation. In the 2nd and 3rd sections of the design, microgrooves and main channels were drawn separately to apply two-step photolithography. Each section has 2 almost identical microchip designs, but the only difference is the size of the inlets. The 8 mm and 2 mm inlets are designed to observe the effects of the different cell

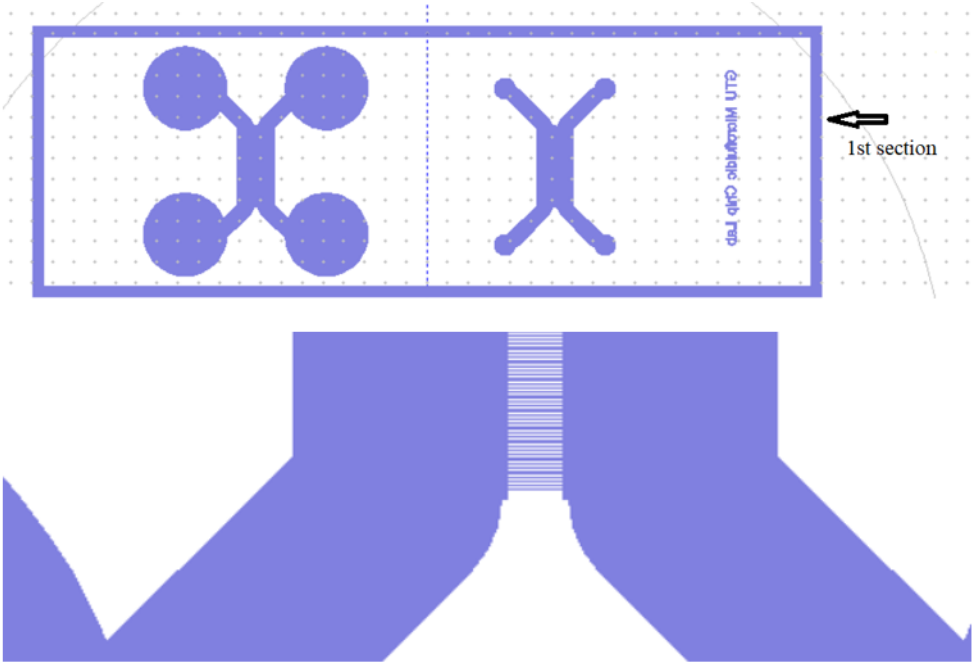

Figure 3.4 1st section of the mask design.

culture methods.

3.1.2 Photomask Writing And Preparation

Designed patterns were printed on the commercial 5-inch chrome photomask (Nanofilm) by using HEIDELBERG DWL 66 fs laser lithography system in the clean-room of Gebze Technical University. This photomask has a 100 nm Chrome layer which is coated by a 500 nm AZ1505 positive photoresist on the top.

After the printing process, the photomask was kept in the AZ726 MIF developer for 60 seconds to clear the areas which were exposed to the laser light. Following the development, the mask was immersed in the Cr etcher solution for 100 seconds. The patterns were checked under a light microscope. Since all the patterns were clearly seen under the microscope, remover was used to clean the remaining photoresist material from the mask. AZ100 remover was used for 10 minutes at 80 °C to remove the excessive material. As the last step, the mask was rinsed with D.I. water and dried with N_2. Mask was checked under the light microscope again to make sure it is clean

enough. A photo of the mask was demonstrated in Figure 3.5 below.

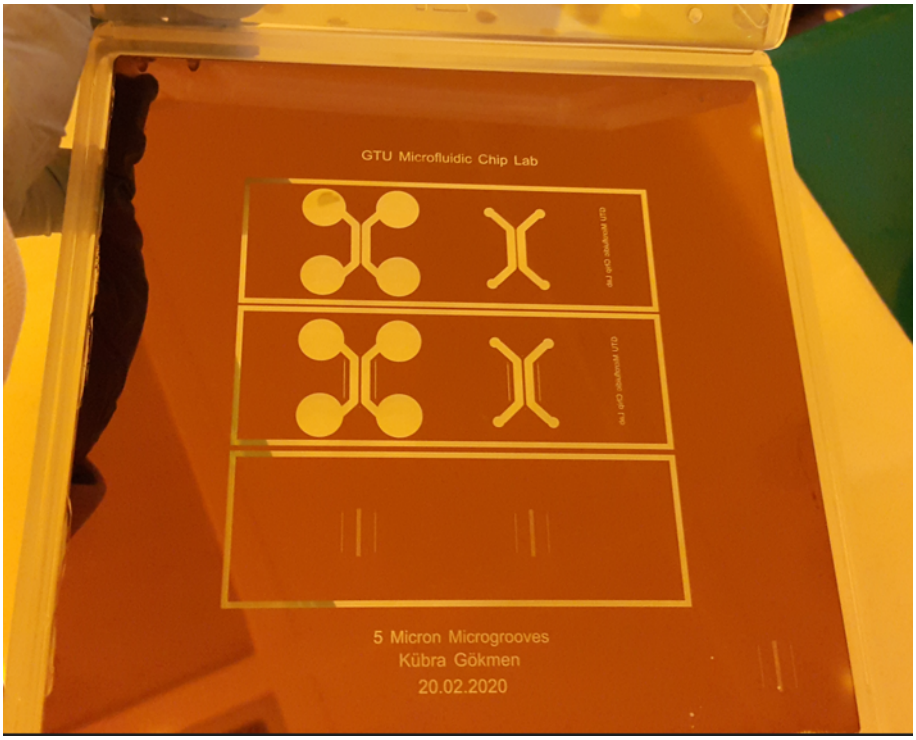

Figure 3.5 Photo of the mask.

3.1.3 Preparation of SU-8 Master Molds on Si/SiO_2 Wafers

Different types of master molds were prepared to compare and observe the effects on the cell culture experiments. Two-step photolithography was applied to obtain structures at different heights. SU-8 2005, SU-8 2050, SU-8 3005, and SU-8 3050 negative photoresists were supplied by Kayaku Chemicals to carry out the photolithography process. Properties of different master molds were listed below.

1. Preparation with SU-8 3005 and SU-8 3050 to see the effect of UV exposure dose on microgroove width by using SÜSS Mirotech MJB4 Mask Aligner.

2. Preparation with SU-8 2005 and SU-8 2050 to see the effect of UV exposure dose on microgroove width by using SÜSS Mirotech MJB4 Mask Aligner.

3. Preparation with SU-8 3005 and SU-8 3050 to have a similar microgroove width

with the first part by using UV-EX Pioneer Lithography System from Mikronya Lithography Systems Ltd.

Master molds which were prepared in the first and third steps were used to fabricate microfluidic chips with 2 mm and 8 mm inlets to see the effects on the cell culture studies.

3.1.3.1 Preparation of the Master Molds With SU-8 3000 Series. Processing steps suggested in the datasheet of SU-8 3000 series supplied by Kayaku Chemicals have been followed to obtain the microgroove and main channel structures with thickness of 5 μm and 100 μm, respectively. 2 inch Si/SiO_2 wafers and a small rectangular Si/SiO_2 wafer pieces were used for preparing the different master molds. While all parameters were kept constant for each sample, only UV exposure time was changed. Optimum UV exposure time was tried to be determined for obtaining the required microgroove width at this part of the experiment.

- Si/SiO_2 wafers were cleaned in an ultrasonic bath for 5 minutes by keeping them in acetone and IPA, respectively. Si/SiO_2 wafers then were dried with nitrogen gas (N_2), and were placed on a hot plate at 95 °C for 3 minutes to eliminate water or other molecules that may remain on the surface. Si/SiO_2 wafers were kept in a room temperature for cooling down before the photoresist coating.

- Cleaned Si/SiO_2 wafers were placed on the center of a spin coating device for the first layer coating as demonstrated in Figure 3.6 below. 1 mL of SU-8 3005 negative photoresist for each inch (25 mm) of substrate diameter was dispensed on the cleaned Si/SiO_2 wafers surface and coating was applied according to the recipe that was suggested in the datasheet of SU-8 3005. In the first step, the coated Si/SiO_2 wafers were spun at 500 rpm for 10 seconds with an acceleration of 100 rpm/second which was followed by spinning at 3000 rpm for 30 seconds with the acceleration of 300 rpm/second as a second step.

Figure 3.6 Spin coating of the first layer.

- Photoresist coated Si/SiO_2 wafers were kept on the hot plate at 95°C for 2,5 minutes for the soft bake stage. After baking, Si/SiO_2 wafers were kept in a room temperature for 2 minutes.

- After that, coated Si/SiO_2 wafer and designed Cr mask were placed in a mask alignment system (KARL SUSS-MJB4 mask aligner) which has a UV light source (365nm) with 21 mW/cm^2 power. SU-8 coated Si/SiO_2 wafers were exposed to UV light through the photomask by using hard contact mode for 5,4,3 and 2 seconds, respectively.

- Cured Si/SiO_2 wafers were placed on a hot plate directly after the UV exposure for post exposure bake stage. They were kept on the hot plate at 65°C for 1 minute and then at 95°C for 1,5 minutes.

- Samples were kept at room temperature for a few minutes to cool down before the

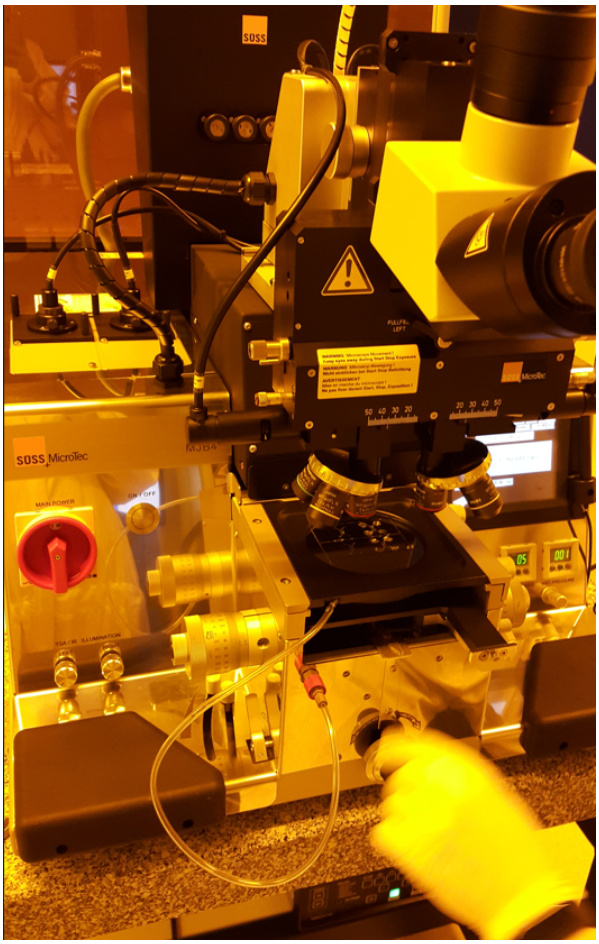

Figure 3.7 UV exposure for the first layer.

development stage. Cooled SU-8 coated Si/SiO_2 wafers were immersed into Mr-Dev-600 developer and kept for 1,5 minutes to remove the uncured SU-8 polymer. Substrates were washed with IPA and dried with N_2 gas.

- Finally, the samples were hard baked at 150 °C for 5 minutes to improve resistance. Microgroove sizes were measured using an optical microscope.

- After measurement of the microgroove sizes, samples were placed on the spin coater again for the 2nd layer coating. 1 mL of SU-8 3050 negative photoresist for each inch (25 mm) of substrate diameter was dispensed on the Si/SiO_2 wafer and coating was applied according to the recipe that was suggested in the SU-8 3050 datasheet. In the first step, a rotating speed of 500 rpm was implemented by increasing the speed in 100 rpm steps gradually for 10 seconds and it was followed by the second step which applied the rotating speed of 2000 rpm for 30

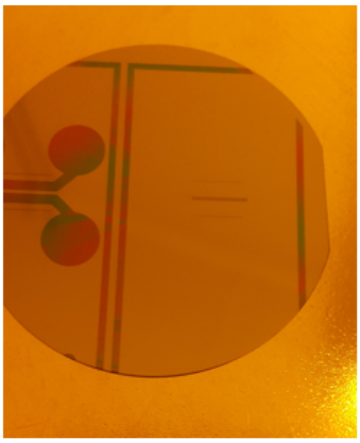

Figure 3.8 SU-8 on Si/SiO_2 wafer after the first development.

seconds in increments of 300 rpm.

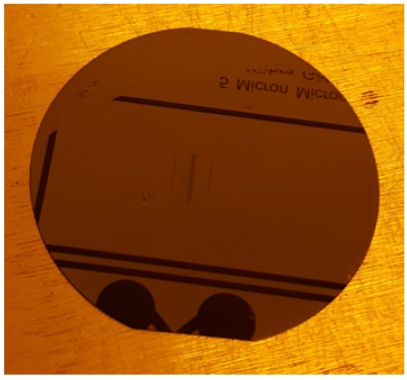

Figure 3.9 Soft bake after second layer coating of SU-8 3050.

- Same steps in the first layer coating process were followed by changing the parameters. Si/SiO_2 wafers were soft-baked at 95 °C for 35 minutes, and they were cooled down to room temperature and kept for 15 minutes for relaxation. After that, they were exposed to UV light for 11 seconds in the same mask alignment system.

- Samples were heated on the hot plate at 65 °C for 1 minute and then at 95 °C for 5 minutes.

- After cooling down of SU-8 coated Si/SiO_2 wafers, they were developed for 13 minutes with an additional 2 minutes in an ultrasonic bath. After they were

rinsed with IPA and dried with Nitrogen gas, samples were checked by the optical microscope.

- As the last step, master molds were hard baked at 150 °C for 5 minutes to improve the mechanical strength.

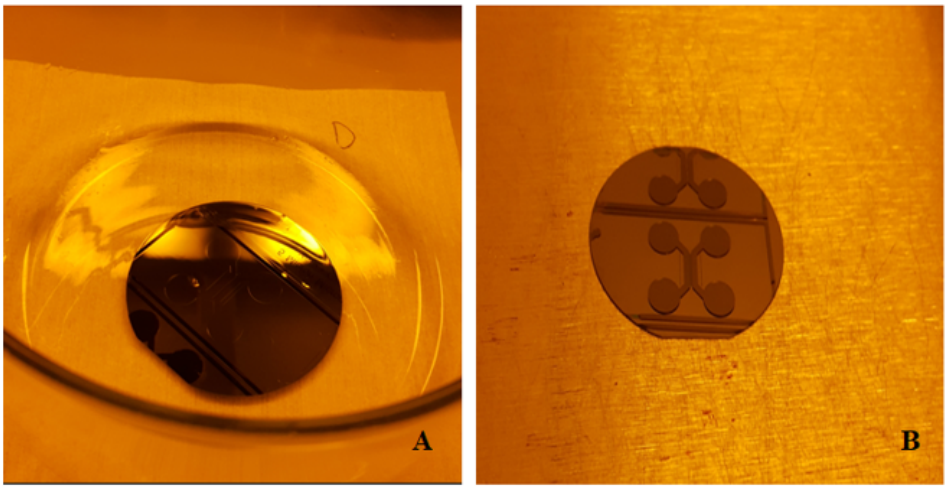

Figure 3.10 (A) Development after 2nd UV exposure (B) Hard bake after 2nd development.

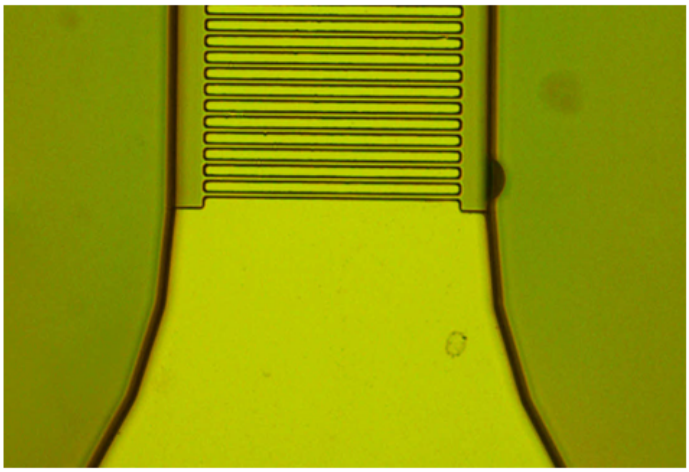

Figure 3.11 Microscope image after 2nd development (Magnification factor: 10x)

3.1.3.2 Preparation of the Master Molds With SU-8 2000 Series. In this part, master molds were prepared by using the SU-8 2000 negative photoresist series.

For the first layer, SU-8 2005 photoresist was used and optimum microgroove size was tried to obtain by changing the UV exposure time. SU-2050 photoresist was used for coating the second layer.

Application steps were the same as the 1st and 2nd master molds preparation. 2 inch Si/SiO_2 wafers were used and production steps were followed by changing the variables according to SU-8 2005 datasheet. Details of the application steps were demonstrated in Table 3.1 below. Microgroove sizes in all samples were measured after the first layer of coating. Different microgroove widths were obtained depending on the UV exposure time.

Table 3.1
Preparation steps of the master molds by using SU-8 2000 photoresist series.

Preparation Steps	**1st layer coating with SU-8 2005 (for $\approx$ 5 μm thickness)**	**2nd layer coating with SU-8 3050 (for $\approx$ 120 μm thickness)**
Spin coating	-500rpm for 10 sec (100rpm ramp) -3000rpm for 30 sec (300rpm ramp)	-500rpm for 10 sec (100rpm ramp) -1500rpm for 30 sec (300rpm ramp)
Soft Bake	At 95 °C for 2 minutes	First at 65°C for 5 minutes, Second at 95 °C for 22 minutes
Relaxation Time	2 minutes	15 minutes
UV Exposure	21mW/cm^2 power for 5,4,3,2 seconds with vacuum contact	21mW/cm^2 power for 13 seconds
PEB	-At 95 °C for 3 minutes	First at 65 °C for 5 minutes, Second at 10 °C for 5 minutes
Development, Rinse and Dry	1 minute development followed by IPA rinsing and N_2 drying	13 minutes of development followed by IPA rinsing and N_2 drying
Hard Bake	At 150°C for 5 minutes	At 150°C for 5 minutes

3.1.3.3 Preparation of the Master Mold With Different UV Light Source.

2 inch Si/SiO_2 wafer was coated with SU-8 3005 and SU-8 3050 photoresists in this part of the experiment. The same application steps in part 3.1.3.1 were applied by

changing only the UV light source and first layer spin coating properties.

A UV-EX Pioneer Lithography System (Mikronya Lithography Systems Ltd.) in the Microfluidic Chip Laboratory at Gebze Technical University was used as a UV light source for producing the first layer of the master mold. The second layer photolithography application was made in the cleanroom because of the alignment requirements. The details of the preparation steps were demonstrated in Table 3.2 below.

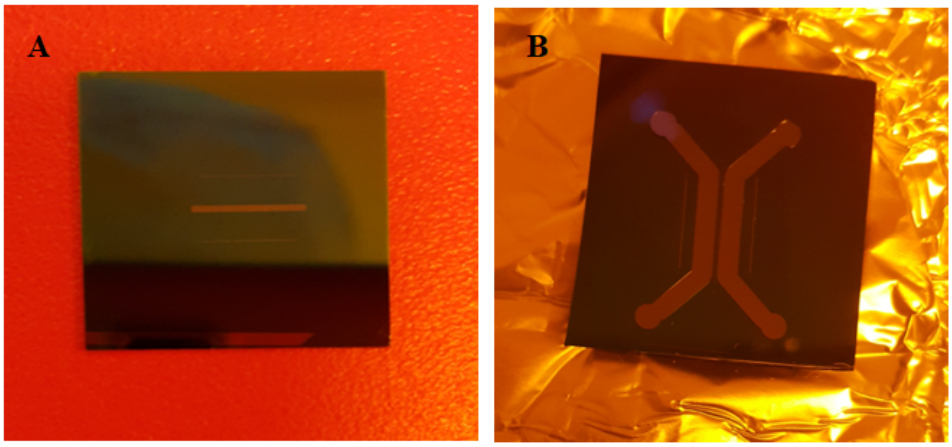

Figure 3.12 Rectangular substrate images (A) After first development (B) After second development.

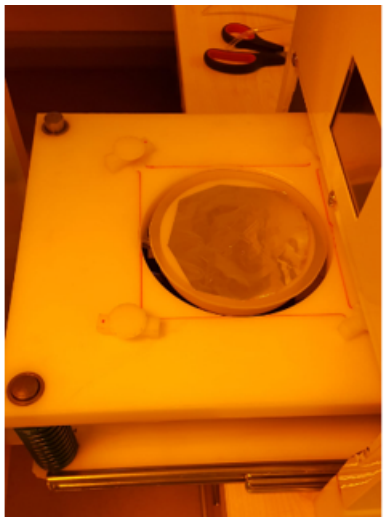

Figure 3.13 UV-EX Pioneer Lithography System in Microfluidic Chip Laboratory at GTU.

Table 3.2
Preparation steps of the master mold by using SU-8 3000 photoresist series with a different light source.

Preparation Steps	**1st layer coating with SU-8 3005 (for ≈ 4 μm thickness)**	**2nd layer coating with SU-8 3050 (for ≈ 100 μm thickness)**
Spin coating	-500rpm for 10 sec (100rpm ramp) -4000rpm for 30 sec (300rpm ramp)	-500rpm for 10 sec (100rpm ramp) -2000rpm for 30 sec (300rpm ramp)
Soft Bake	At 95 °C for 2,5 minutes	At 95 °C for 35 minutes
Relaxation Time	2 minutes	15 minutes
UV Exposure	58 mW/cm^2 power for 4 seconds with vacuum contact	21 mW/cm^2 power for 11 seconds
PEB	First at 65 °C for 1 minute, Second at 95 °C for 1,5 minutes	First at 65 °C for 1 minute, Second at 95 °C for 5 minutes
Development, Rinse and Dry	1,5 minutes of development followed by IPA rinsing and N_2 drying	13+2 (in UB) minutes of development followed by IPA rinsing and N_2 drying
Hard Bake	At 150 °C for 5 minutes	At 150°C for 5 minutes

3.1.4 Preparation of the PDMS Negative Templates

In this part of the experiment, the soft lithography technique was implemented to prepare the PDMS negative templates. PDMS (Sylgard 184 silicone elastomer and curing agent) is supplied by Dow Silanes and silicone elastomer was mixed homogeneously with the curing agent at a w/w ratio of 10:1 for 10 minutes. The mixture was kept in the vacuum desiccator for about 40 minutes to eliminate the bubbles.

Aluminum foil was placed in a 6 cm glass petri dish to form an outer template for 2-inch master molds. Master molds were placed into an aluminum foil template as demonstrated in Figure 3.14 below. On the other hand, the rectangular master mold was directly placed in the 6 cm petri dish without using an aluminum foil template as demonstrated in Figure 3.15. PDMS mixture was poured on master molds carefully. Then they were kept on the hot plate at 80 °C for 1 hour for curing. 3 different master

molds were used for PDMS casting.

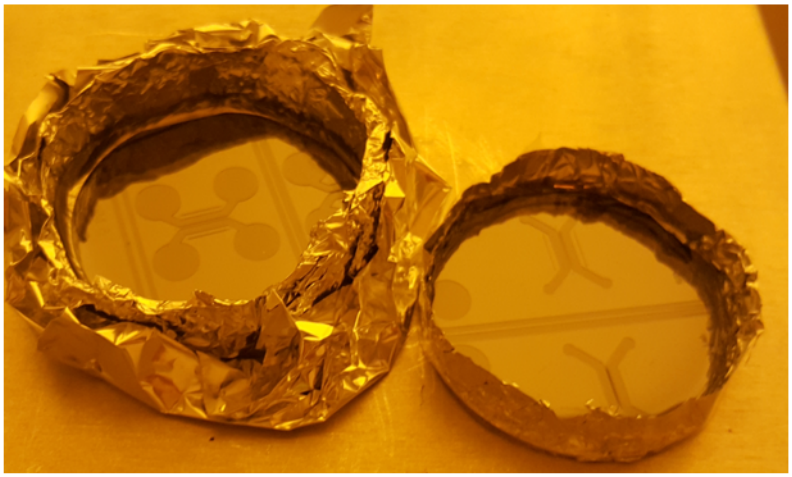

Figure 3.14 PDMS curing on SU-8 master molds.

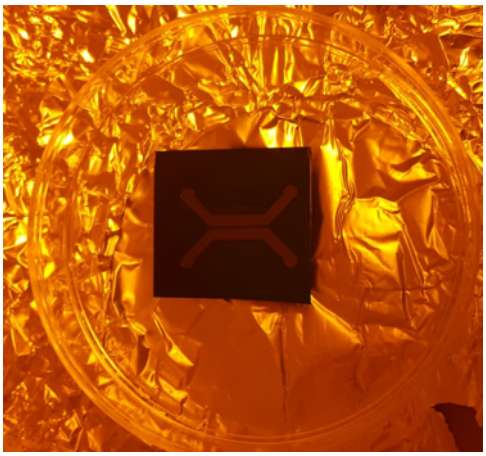

Figure 3.15 Master mold placed in a glass petri dish for PDMS curing.

After curing stage, cured PMDS mold was cooled down for about 60 minutes at room temperature. PDMS negative template was slightly peeled off from the master mold with the help of surgical blade. While some of PDMS molds were directly peeled off from the master mold, others were treated with trimethylchlorosilane vapor to decrease the adhesion between the PDMS mold and SU-8 master mold. SU-8 master molds and a few drops of trimethylchlorosilane in an open glass petri dish were kept in a desiccator for 40 minutes at room temperature to cover the SU-8 surface [76, 77]. PDMS mold containing the microchannels was cut off to have the final microfluidic chip. 2 mm and 8mm biopsy punches were used to obtain inlets for cell culture applications.

3.1.5 Packaging of Microfluidic Chips by Plasma Cleaning

PDMS mold was cleaned before plasma bonding. Firstly, Scotch brand vinyl tape was used to remove any dust from PDMS surface. Then, PDMS mold was held with tweezers and washed with D.I. water. It was sonicated in D.I. water for 5 minutes by placing it in a glass petri dish then it was rinsed with D.I. water a few times. After that, it was sonicated in 70 % EtOH for 5 minutes and was rinsed with 70 % EtOH twice. After the cleaning process PDMS mold was dried with N_2. The cleaned PDMS negative template was placed in a clean glass petri dish by turning the patterned side face up. Petri dish was covered with a clean aluminum folio including small holes and was kept in a laminar hood for 15 minutes to dry completely. Scotch tape was covered on the patterned side of the mold after the drying process to eliminate any dust to attach and remove the remaining debris.

The cover glass was cleaned with acetone and IPA for 5 minutes respectively and was dried with nitrogen gas. Cleaned cover glass and PDMS negative template were placed by facing up the patterned side of the template in a plasma cleaner chamber of PTL-VM500 vacuum plasma treatment system at GTU and waited for 2 minutes ($\approx 10^{-1}$ mbar at room temperature) for plasma turning the surfaces hydrophilic and providing permanent bonding.

Figure 3.16 Plasma cleaning with PTL-VM500 vacuum plasma treatment system at GTU.

Plasma-treated surfaces of the cover glass and PDMS mold were contacted each other immediately after the plasma treatment by applying a slight pressure to help bonding. The chip was kept on a 65°C hot plate for 30 minutes by putting a light weight on it to provide better bonding.

Figure 3.17 Heating after plasma cleaning.

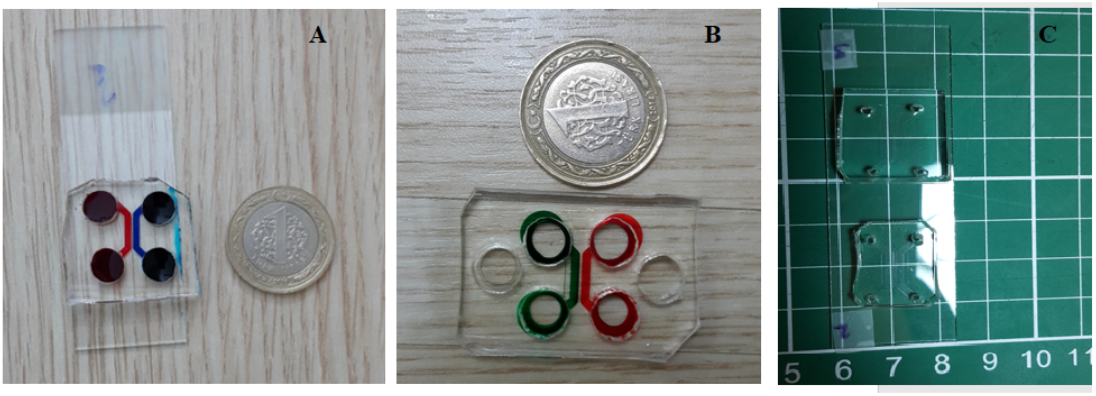

Figure 3.18 (A) Microfluidic chip with 8 mm inlets (B) Microfluidic chip with 8 mm inlets including extra reservoirs for water (C) Microfluidic chips with 2 mm inlets

.

Scotch brand vinyl tape was used to cover the surface and inlets of the microfluidic chips and kept in a closed petri dish until cell culture experiments. Since PDMS easily turns back to its hydrophobic structure in a short time when it is exposed to air [54], it is important to cover the reservoirs.

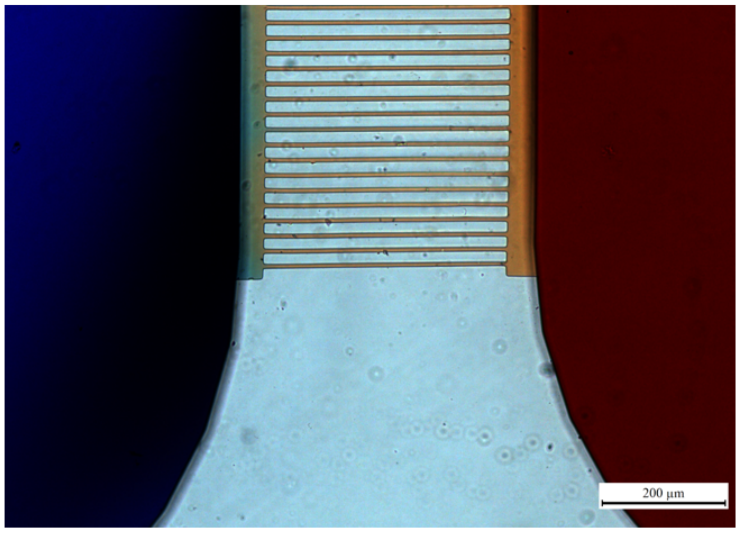

Figure 3.19 Microscopic image of the microfluidic chip after channel staining.

3.2 Sterilization

The outer and inner surfaces of the microfluidic chips and Petri dishes were rinsed with 70 % EtOH and they were placed into the laminar hood. The liquid on the surface and in the reservoirs of the chip was aspirated and channels were washed with 70 % EtOH for twice. Microchannels were filled with fresh 70 % EtOH and enough amount of 70 % EtOH was added to the petri dish to cover the whole microfluidic chip surface. After 15 minutes, 70 % EtOH was aspirated from the inner channels and outer surfaces of the chips. Inner channels were washed with 70 % EtOH twice again and they were filled with 70 % EtOH to let them wait for additional 5 minutes. EtOH was aspirated from the channels and chips were left in the hood for a few minutes to dry. Microfluidic chips were exposed to UV light for 15 minutes and they were transferred to the sterile Petri dishes as a last step of the sterilization.

3.3 Cell Culture Studies

3 different microfluidic chip models were used for cell culture studies. SH-SY5Y neuroblastoma cells were cultured in microfluidic chips to observe the cell migration to

the other microchannel and the separation of axons from the somas. Cells were loaded by using filtered micropipette tips in the first method, and directly through the wide reservoirs with 8 mm diameter in the second method. The cross-sectional views of the fabricated microfluidic chips were demonstrated in Figure 3.20 below.

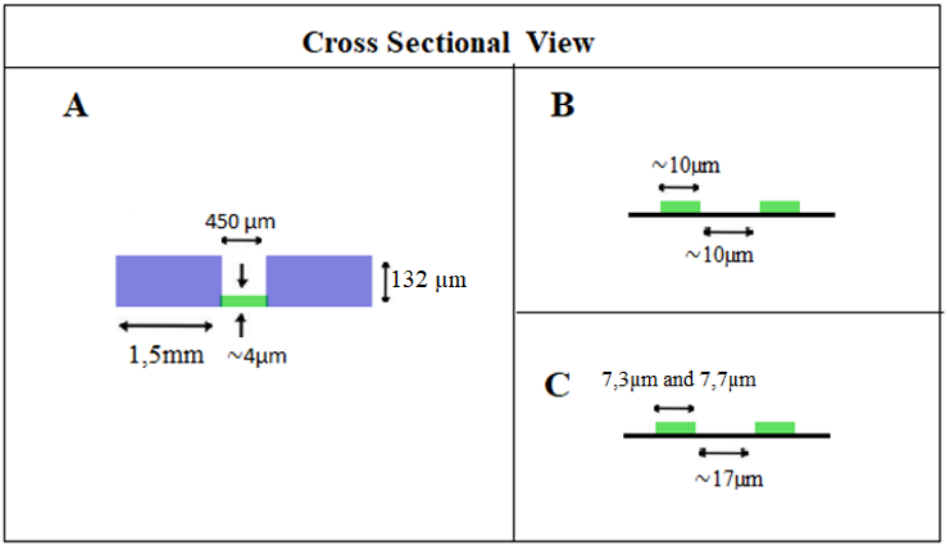

Figure 3.20 Schematic representation of fabricated chips. (A) Cross-sectional view of the main channels and microgrooves demonstrating the length and thickness. Cross-sectional side view of large (B), small (C) microgrooves.

3.3.1 Cell Seeding With Filtered Micropipette Tips

Microfluidic chips which have 2 mm inlets with a width of 7.3 μm microgrooves and 10.2 μm microgrooves were used for cell seeding and the effect of microgroove width on cell migration was observed. 1000 μm filtered micropipette tips were used for static cell seeding and changing the medium. After sterilization, 200 μL phosphate-buffered saline (PBS) was filled into the right channels and it was waited for a few minutes to fill the microgrooves. Then, the left channels were filled with PBS. After PBS wash, channels were aspirated, and then 200 μL of 0.1 mg/mL poly L-lysine (PLL) solution was added with filtered pipette tips into each channel, and chips were placed in an incubator at 37 °C for 1 h for providing effective coating. After 1 hour, the PBS wash step was repeated 2 times to remove the excess PLL. Channels were filled with cell culture media and chips were placed in an incubator at 37 °C until the

cells were ready. RPMI 1640 (Pan Biotech, Germany) supplemented with 10 % FBS (fetal bovine serum) (ATCC 30-200TM), and 1 % penicillin-streptomycin (Biosera, 45 Nuaille, France) were used for the routine cell culture process of SH-SY5Y cells.

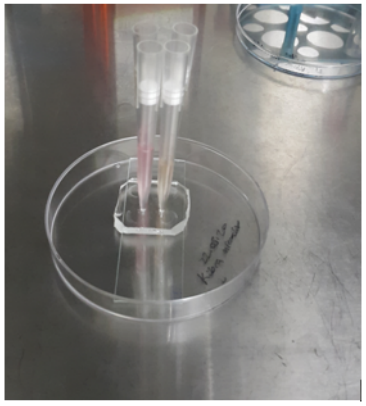

Figure 3.21 Digital image of the microfluidic chip with 2 mm inlets before cell culture change.

SH-SY5Y cell suspension was prepared with the density of 2x10^5 cells/mL from the 11th passage of the cells. An empty 1000 μm filtered micropipette tip was fixed to the lower left inlet while the other pipette tip was filled with 1000 μL cell suspension which was then placed in the upper left inlet. The cell suspension was loaded to the left channel by slightly pressing the micropipette and the same pressure was used until the pipette tip in the lower left inlet was filled with cell suspension with the same level. Cells were kept in the culture hood for 5 minutes for the attachment. After that, the right channel was filled with fresh culture medium by using the same steps with cell loading. After checking the cells through an optical microscope, microfluidic chips were placed in an incubator with humidified 5 % carbon dioxide (CO_2) atmosphere at 37 °C. Pipette tips and culture media were changed at the 96th hour. A digital image of the microfluidic chip before the cell culture change was demonstrated in Figure 3.21 above.

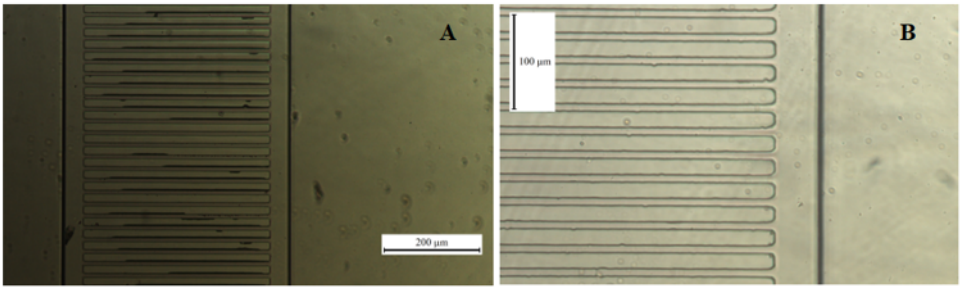

Figure 3.22 Microscope image of microfluidic chips before cell culture (A) Chip with smaller (7.3 μm) microgrooves (B) Chip with larger (10.2 μm) microgrooves.

3.3.2 Cell Seeding Through Wide Reservoirs With 8 mm Diameter

Two different microfluidic chips containing 7.7 μm and 10.2 μm width microgrooves were used in this part of the experiment. The main difference from the chips used for the first cell culture technique was the size of the inlets. The chips with 8 mm diameter inlets were used for the cell culture process by using the inlets as reservoirs for the culture media. Cell seeding and culture media change were processed through the reservoirs in a static environment. Some of the microfluidic chips were placed angled in a petri dish and waited for 5 minutes in the incubator after cell seeding to place the cells closer to the microgroove openings.

The cell seeding process in the study sponsored by Xona Microfluidics was followed by modifying some steps [78]. After the sterilization process, 150 μL PBS was added to the upper left reservoir and waited for 1,5 minutes to allow it to flow through the main channel. Then another 150 μL PBS was added to the lower left reservoir and it was waited for 5 minutes for providing liquid to reach the microgrooves and flow through them. 150 μL PBS was added to the upper right and lower right reservoirs respectively and the chips were left in the hood for 10 minutes.

After PBS wash, channels were coated with 0.1 mg/mL poly L-lysine (PLL). 100 μL PLL solution was added to the upper left reservoir and after 1,5 minutes another 100 μL PLL solution was added to the lower left reservoir. It was repeated for the

right channel too. Then microfluidic chips were placed in an incubator at 37 °C for 1 hour for coating. Microchannels were washed with PBS for 2 times as mentioned above to eliminate the PLL excess. Then, the chips were filled with fresh culture media by following the same steps with PLL coating, and they were kept in the incubator at 37 °C until the cells were ready.

Figure 3.23 Microfluidic chip with 8 mm inlets in a cell culture hood during cell seeding.

SH-SY5Y cell suspension was prepared with a density of $\approx 12\times10^6$ cells/mL. The majority of culture media was moved from the reservoirs by aspirating the liquid away from the main channels to leave the media in the channels. 5 μL of cell suspension was loaded to the upper left reservoir and another 5 μL of cell suspension was loaded to the lower left reservoir (totally $\approx$ 120.000 cells) by placing the pipette tip close to the main channels. Some of the chips were placed angled in the hood to direct the cells closer to the microgrooves. All chips were kept in the hood for 5 minutes to provide cell attachment.

Two-step cell loading method was tried to keep more cells in the main channels and prevent them from moving to the reservoirs. After loading 5 μL cell suspension from each upper and lower left reservoir with the density of $\approx 6\times10^6$ cells/mL, they were kept in the hood for 5 minutes for cell attachment. This step was repeated for the second loading to have around 120.000 cells in total. After cell attachment cells were checked under the microscope. 150 μL culture media was added to each of the upper left and lower left reservoirs and then it was repeated for each reservoir on the right. 1,8 mL cryovials were filled with autoclaved water and vials were placed in a petri dish

next to the microfluidic chips with the lid open to prevent evaporation. Chips were placed in an incubator with humidified 37 °C 5 % carbon dioxide (CO_2) atmosphere at 37 °C. Culture media was changed every 24 hours for 7 seven days.

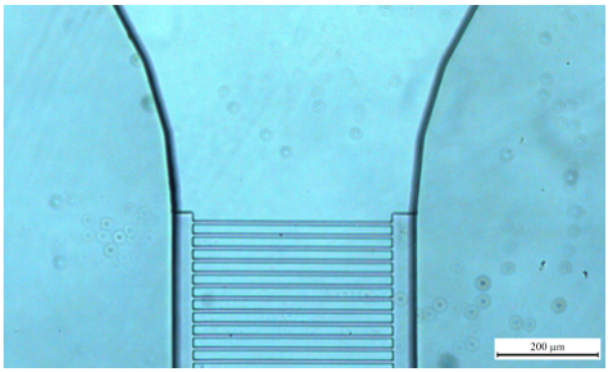

Figure 3.24 Microscope image of the microfluidic chip with 7.7 μm width microgrooves before cell seeding.

4. RESULTS

4.1 Microfluidic Chip Fabrication Results

Different master molds were prepared by using SU-8 negative photoresists in different viscosities. SU-8 2005 and SU-8 3005 photoresists were used by changing the UV exposure time to observe the effect on the microgroove sizes. Different microgroove widths were obtained as demonstrated in Table 4.1. below.

Table 4.1
Microgroove width results depending on the UV exposure energy and photoresist types.

Microgroove Width			
SU-8 3005 coating (power:21mW/cm^2)	**SU-8 2005 coating (power:21mW/cm^2)**	**SU-8 3005 coating (power:58mW/cm^2)**	**UV exposure time**
15 μm	13.7 μm	-	5 seconds
10.2 μm	10.2 μm	7.7 μm	4 seconds
7.3 μm	8.6 μm	-	3 seconds
7.5 μm	8.5 μm	-	2 seconds

Smaller microgroove sizes were obtained by decreasing the UV exposure time. It was observed that 2 seconds of exposure time was not enough because of inefficient cross-linking and damaging the microgroove structures during development. While similar results were obtained with different photoresist types, minimum microgroove width was obtained by using SU-8 3005 photoresist type. Microgroove widths of two different master molds which were produced by using SU-8 3005 and applying different exposure doses were demonstrated in Figure 4.1 below. These molds were used to fabricate microfluidic chips for cell culture studies. Microscope images of the microgroove widths obtained by using SU-2005 after applying different UV exposure doses were shown in Figure 4.2 below. In addition to that, similar microgroove width (7.7 μm), which was demonstrated in Figure 4.3, could be obtained with SU-8 3005 with a diffrent UV light source.

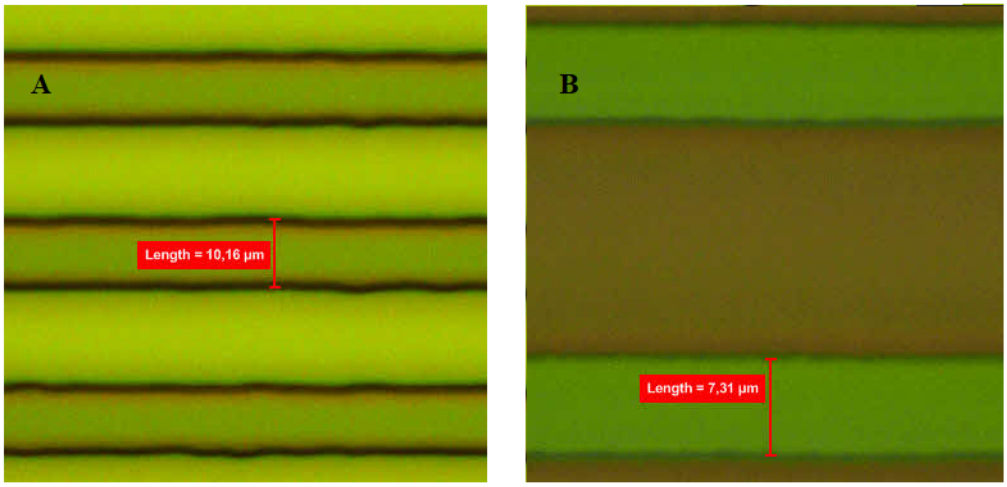

Figure 4.1 Microgroove width measurement under microscope (A) Patterns obtained with SU-8 3005 coating after applying exposure energy of 84 mJ/cm^2 (21 mW/cm^2 power for 4 s) (magnification factor: 50x) (B) Patterns obtained with SU-8 3005 coating after applying exposure energy of 63 mJ/cm^2 (21 mW/cm^2 power for 3 s) (magnification factor: 100x).

Microgroove depths of the master molds were measured by using a profilometer in the cleanroom at Boğaziçi University. Since spin coating speed was slightly increased, and a different photolithography device was used in the last master mold production; a slight change was observed in the depth of the microgrooves. While $\approx$ 4.4 μm channel depth was obtained in the first production step, $\approx$4 μm channel depth was reached in the production of the last master mold. The values were demonstrated in Figures 4.4 and 4.5 A below. In addition, the main microchannel depth of the microfluidic chip fabricated by using a SU-8 3050 photoresist was also measured by using the same profilometer, and the channel depth was measured as $\approx$ 132 μm which was demonstrated in Figure 4.5 B below.

SU-8 photoresist coating caused some problems during master mold production when trying to get thicker channels. Especially after SU-8 2050 coating, coated substrates stuck to the photomask during UV exposure. To prevent this problem, coated substrates were kept at room temperature for 15 minutes. This modification in the fabrication step helped to get better results. In addition, increasing the temperature gradually in the soft baking process was another solution.

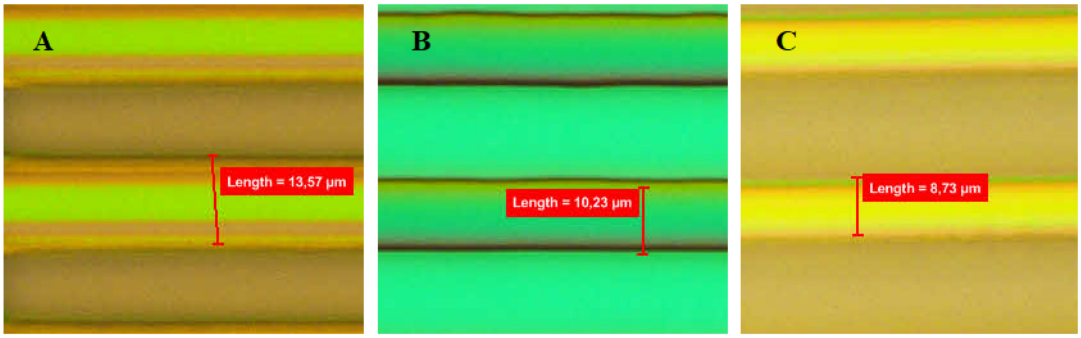

Figure 4.2 Microscope images of microgroove widths were obtained after SU-8 2005 coating. UV exposure (21 mW/cm^2 power) for (A) 5 seconds (B) 4 seconds (C) 3 seconds (magnification factor: 50x).

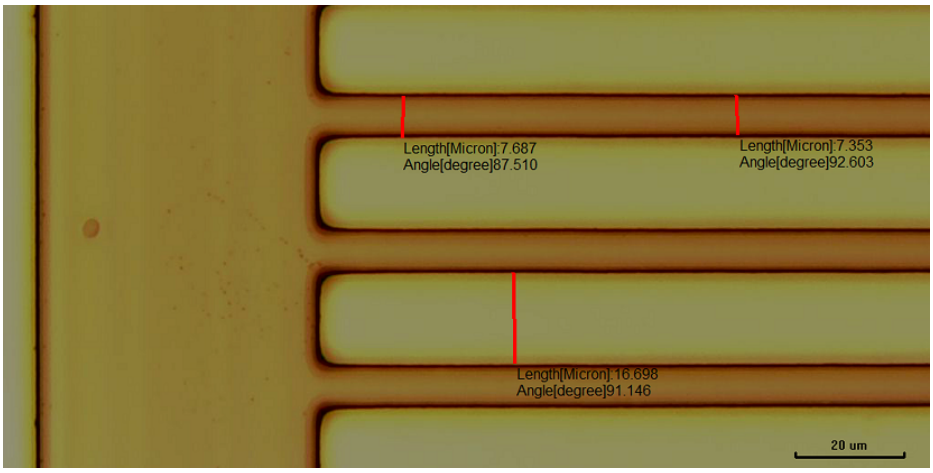

Figure 4.3 Measurement of microgrooves obtained after photolithography with a UV-EX Pioneer Lithography System.

Another problem faced after coating the second layer with SU-8 2050 was the blurring of the patterns obtained after the first development stage. This was an important problem during the alignment of the photomask. To eliminate this problem, one of the alignment markers was colored with AZ1505 positive photoresist material. Although this step provided some help to find the location of alignment marks, microgrooves and alignment marks were not clearly seen under the optical microscope during the alignment. At this point, bigger and more alignment marks in the photomask design would be suggested to improve alignment quality. Colored SU-8 coated Si/SiO_2 wafer before and after the 2nd layer coating was demonstrated in Figure 4.6 below.

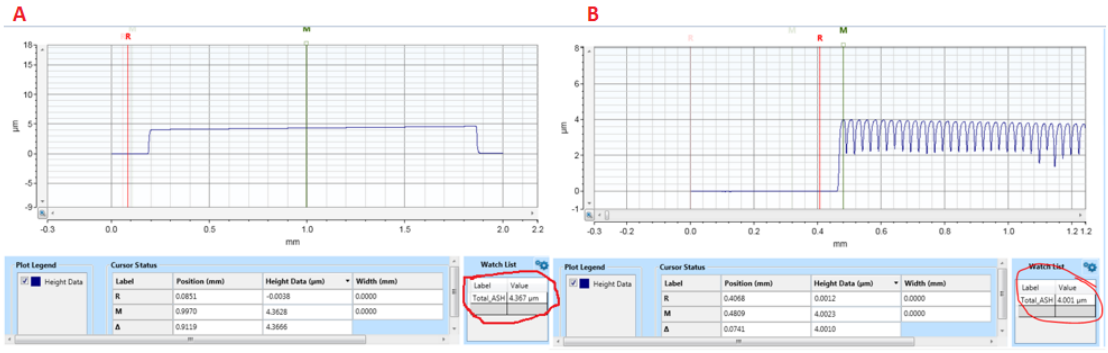

Figure 4.4 Microgroove depth measurement results using a profilometer (A) 7.3 μm microgroove width (B) 7.7 μm microgroove width (Microgroove structures were produced by using SU-8 3005).

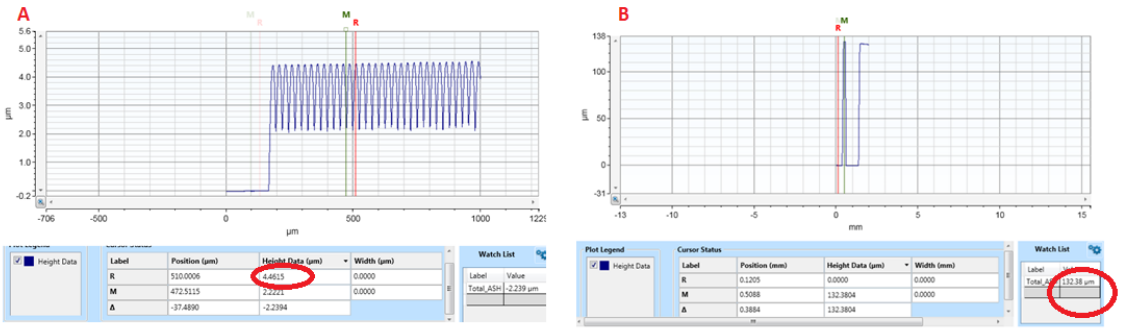

Figure 4.5 (A) Microgroove depth measurement results using a profilometer (10.2 μm width microgroove obtained by using SU-8 3005) (B) Microchannel depth measurement with a profilometer (Microchannel structures were produced by using SU-8 3050).

There were also some challenges during the separation of the PDMS mold from the master mold. It was experienced that some microchannels broke during the peeling off PDMS mold from the rectangular master adhered to the petri dish. Since PDMS was poured onto the rectangular master mold which was placed into the glass petri dish directly without aluminum foil, it caused the master mold to adhere to the petri dish. The applied pressure during the peeling off resulted in broken microgrooves in some areas as it was demonstrated in Figure 4.8. To prevent this, other master molds were placed in aluminum foil templates and it resulted in having final products without a problem. To be able to use the master mold for a longer time, an additional trimethylchlorosilane treatment by using Chemical Vapor Deposition (CVD) method was applied.

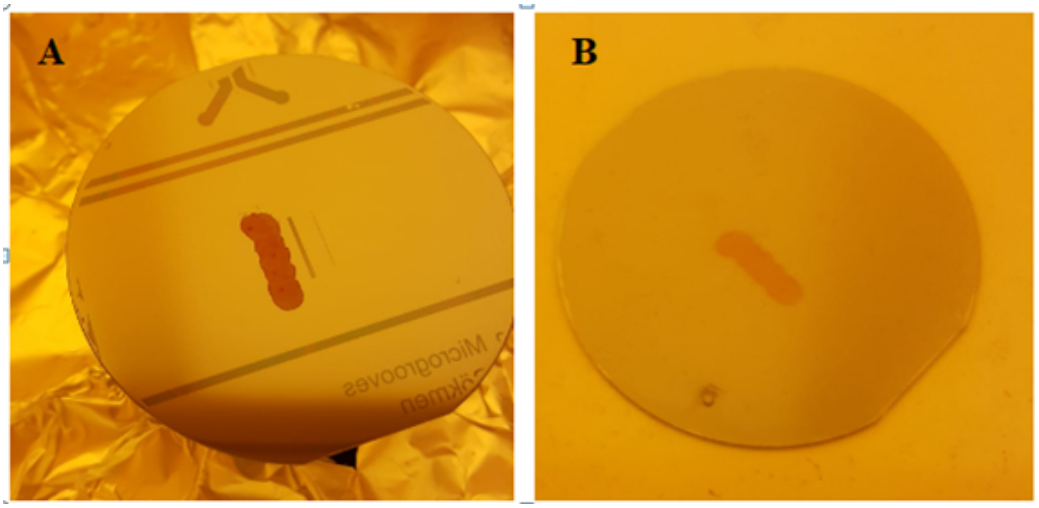

Figure 4.6 AZ1505 photoresist coloring of the alignment markers on the first SU-8 layer on Si/SiO_2 wafer (A) coloring before the 2nd layer coating (B) coloring after the 2nd layer coating.

Figure 4.7 Microscope image of alignment markers (Magnification factor: 5x).

The last problem was related to PDMS bonding to the cover glass. Some microgrooves and supporting units were also bonded to the cover glass because of the pressure applied to the PDMS. It was observed that these bonded structures prevent fluid flow. Applying less and homogenous pressure after plasma treatment helped to solve this problem. The microscope image of the incorrectly bonded structures in the microfluidic chip was demonstrated in Figure 4.9 below.

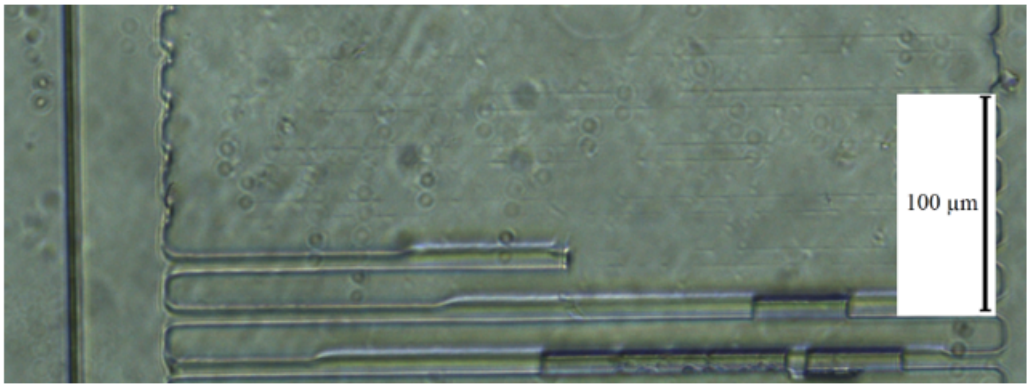

Figure 4.8 Microscope image of the microfluidic chip with broken microgrooves.

Figure 4.9 Incorrectly bonded structures after plasma treatment. Scale bar: 50 μm.

4.2 Cell Culture Results

Cell culture studies by using filtered micropipette tips have been applied on the microfluidic chips with different microgroove widths, respectively 7.3 μm, and 10.2 μm. A different cell culture technique has been applied to the microfluidic chips with 7.7 μm and 10.2 μm microgroove width by opening 8 mm inlets. Optical microscope images were obtained to demonstrate the effects of different cell culture techniques and microgroove widths.

4.2.1 Cell Seeding With a Filtered Micropipette Tip

It has been observed that microgroove width has play an important role in the migration of cells. In figure 4.10, microscope images demonstrated how microgrooves with 10.2 μm width permit the cell migration to the other channel in the same cell culture technique.

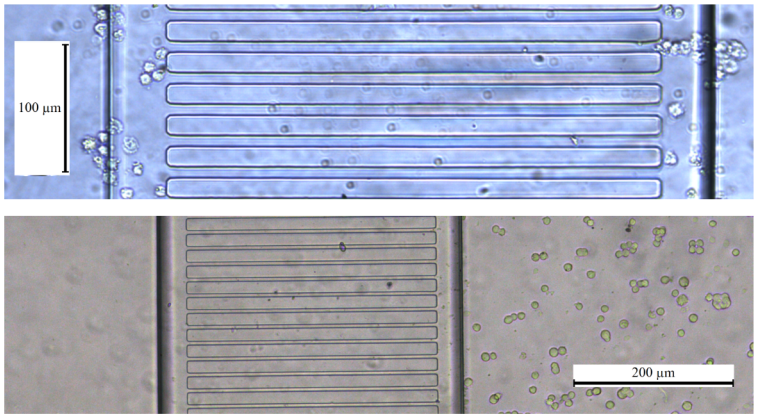

Figure 4.10 Cell migration right after cell loading into the chips with different microgroove widths in cell culture with micropipette tips (A) Microscope image of SH-SY5Y cells cultured in the chip (microgroove width: 10.2 μm) (B) Microscope image of SH-SY5Y cells cultured in the chip (microgroove width: 7.3 μm).

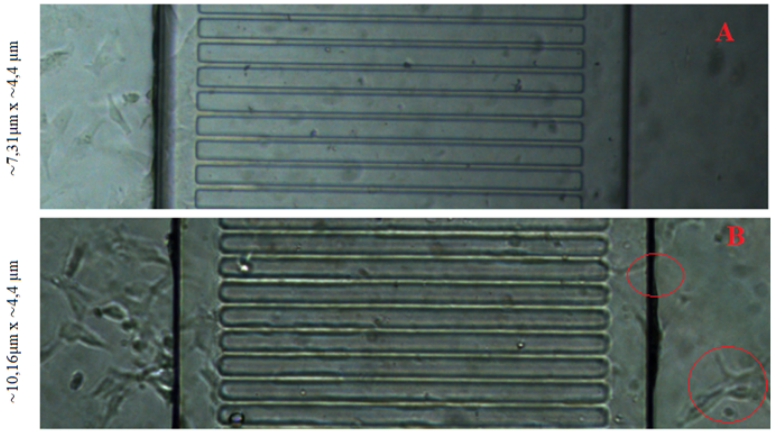

Figure 4.11 Microscope images of SH-SY5Y cells cultured through micropipette tips in different chips after 96 hours. Scale bar: 200 μm (A) Microfluidic chip (microgroove width: 7.3 μm) (B) Microfluidic chip (microgroove width: 10.2 μm).

SH-SY5Y cells which were cultured in microfluidic chips were checked after 96 hours through the optical microscope and attached cells were observed in the right channel of the chip with larger microgrooves in Figure 4.11.B. On the other hand, no

cells were observed in the right channel of the chip in Figure 4.11.A. Since cells were checked right after cell seeding, additional control was required to observe any cell movement happening after the first cell attachment. It proved that no cells migrated to the adjacent channel through a liquid flow that can occur because of any movement, and microgroove size was evaluated enough for a barrier role.

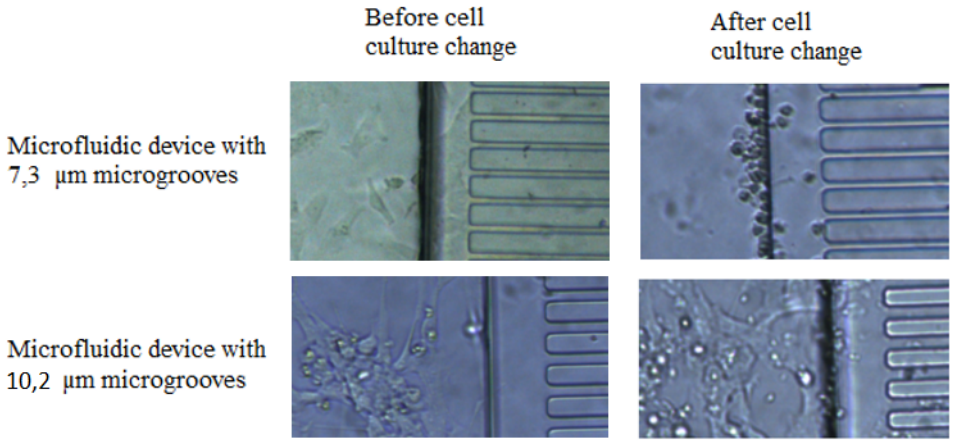

Figure 4.12 Change in cell number and cell attachment after cell culture change on the 4th day. Scale bar: 200 μm.

It was observed that 1000 μm filtered micropipette tips were applied pressure on the cells because of high flow during cell culture change and it affected the cell attachment which caused some of the cells to stay suspended in the chip as demonstrated in Figure 4.12.

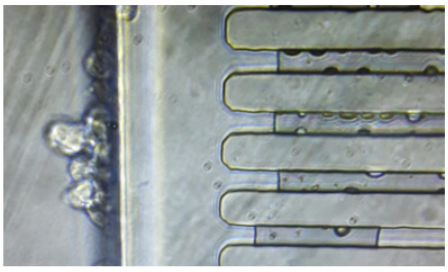

Figure 4.13 Bubble formation in the microgrooves.

Buble formation was observed in the microgrooves during the cleaning of the microchannels and the cell seeding process. It was associated with the high flow rate caused by the pressure created through the pipette tips.

4.2.2 Cell Seeding Through 8 mm Wide Reservoirs

Cell seeding process through 8mm wide reservoirs in microfluidic chips with different microgroove widths which are 7.7 μm and 10.2 μm was demonstrated that cells could not cross to the adjacent channel through 7.7 μm wide microgrooves while there were a few cells observed in the adjacent channel in the chip having 10.2 μm width microgroove. Even though fewer cells could pass through the microgrooves with this method compared to the first cell seeding method, 10.2 μm width of microgrooves was not found suitable for axon isolation. Cell migration images taken through an optical microscope were demonstrated in Figure 4.14 below.

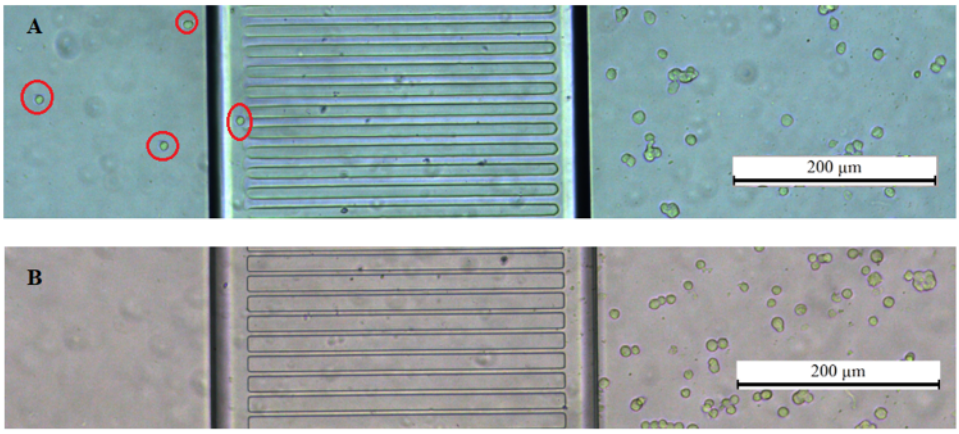

Figure 4.14 Cell migration right after cell seeding into the chips with different microgroove widths through 8 mm wide reservoirs (A) Microscope image of SH-SY5Y cells cultured in the chip with 10.2 μm width. (B) Microscope image of SH-SY5Y cells cultured in the chip with 7.7 μm width.

Table 4.2
Cell migration results depending on the microgroove size and cell culture technique.

Cell culture method	**Microgroove width**	**Microgroove height**	**Cell migration**
Pipette tip method	10.2 μm	4.4 μm	Positive
Pipette tip method	7.3 μm	4.4 μm	Negative
Through 8mm wide reservoirs	7.7 μm	4 μm	Negative
Through 8mm wide reservoirs	10.2 μm	4.4 μm	Positive
Through 8mm wide reservoirs with angle	7.7 μm	4 μm	Negative

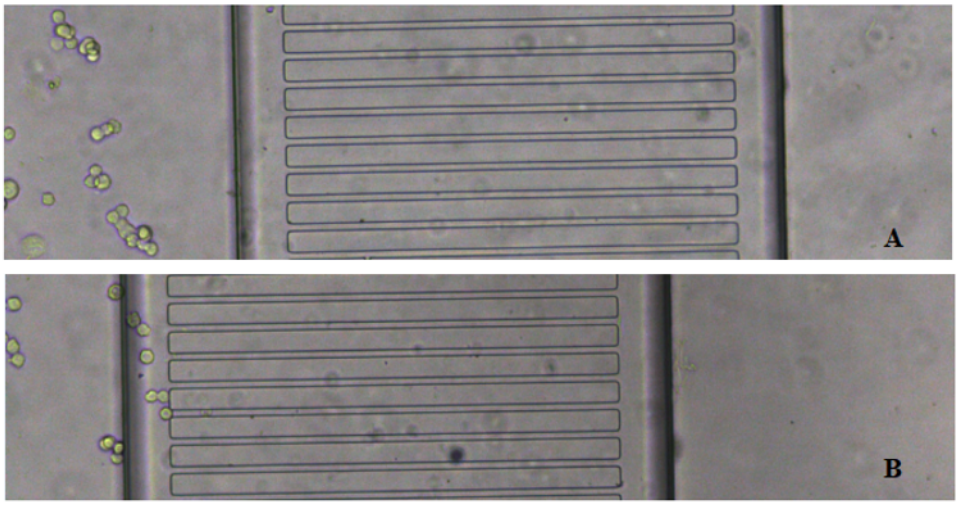

Figure 4.15 Cell positions right after seeding into the microfluidic chips having 7.7 μm width. Scale bar: 200 μm (A) Microfluidic chip positioned without an angle after cell seeding (B) Microfluidic chip positioned at an angle after cell seeding.

After the cell culture experiments through different methods in different microfluidic chips, it was observed that microgrooves with the geometry of 4.4×10.2 μm allow cell migration to the opposite channel while microgrooves having smaller geometry (4.4×7.7 μm) play a barrier role and prevent cells to pass through. Cell migration depending on microgroove size and cell culture method was demonstrated in table 4.2. Since microgrooves 10.2 μm wide didn't prevent cell migration, angled cell seeding and two-step cell seeding methods were not carried out in this microfluidic chip.

Microscope images were taken to demonstrate the effect of chip angel during the cell seeding process. Cells were cultured by giving the chips an angle to direct the cells closer to microgrooves while the other chips with the exact same properties was cultured without an angle. Figure 4.15.B demonstrates that giving an angle to the microfluidic chip for 5 minutes after seeding can direct the cells to the microgrooves. This method can provide better observation of the neurite elongation because of the closeness to the microgrooves. There were no cells detected on the right channels of the chips in both methods which proves that 4×7.7 μm microgroove geometry is applicable to observe the separation of neurites from the somas.

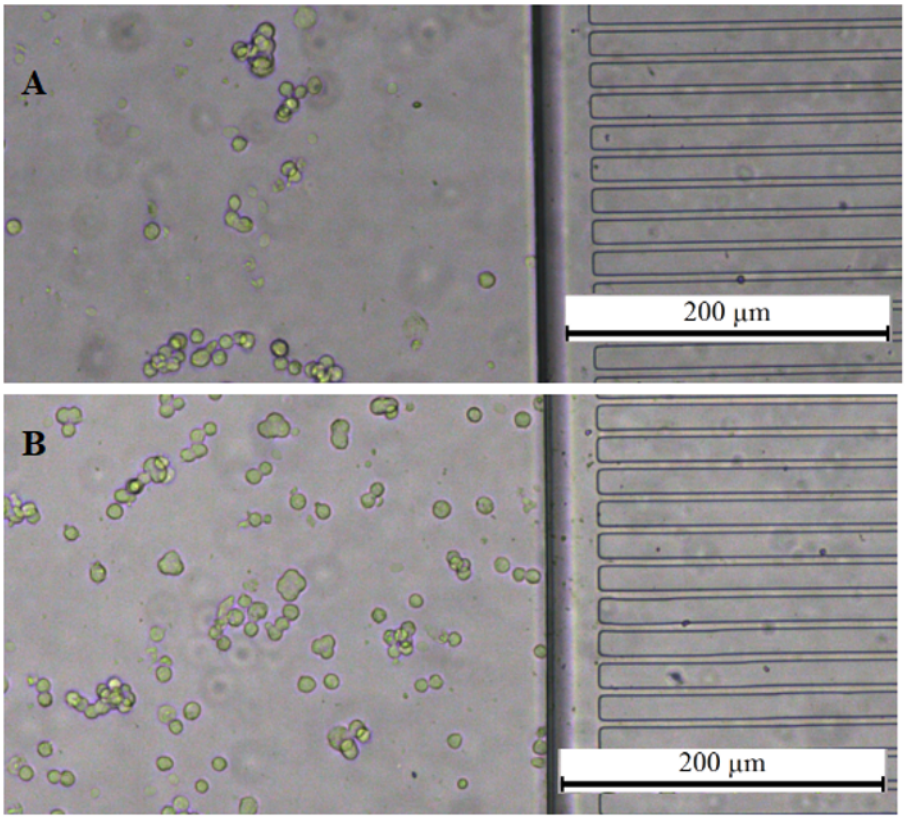

Figure 4.16 Microscope images of cells in the microfluidic chips with 7.7 μm width microgrooves. A) Cells after loading with the first method B) Cells after loading through the two-step loading method.

During the cell seeding process, some cells showed a tendency to move through the main channel and gather around in the opposite reservoir because of the flow. To eliminate this problem, two-step cell loading method was applied as it was mentioned in the experimental method section. This method provided more cells to stay in the main channel compared to the first cell seeding method. In Figure 4.16, the difference between the first method and two-step cell seeding in terms of the number of cells was demonstrated.

Neurite elongation of SH-SY5Y cells through microgrooves was observed on the 3rd day of cell culture. Figure 4.17 demonstrates that cell medium change does not affect cell growth in a negative way and cell growth continues for 7 days without contamination by this method.

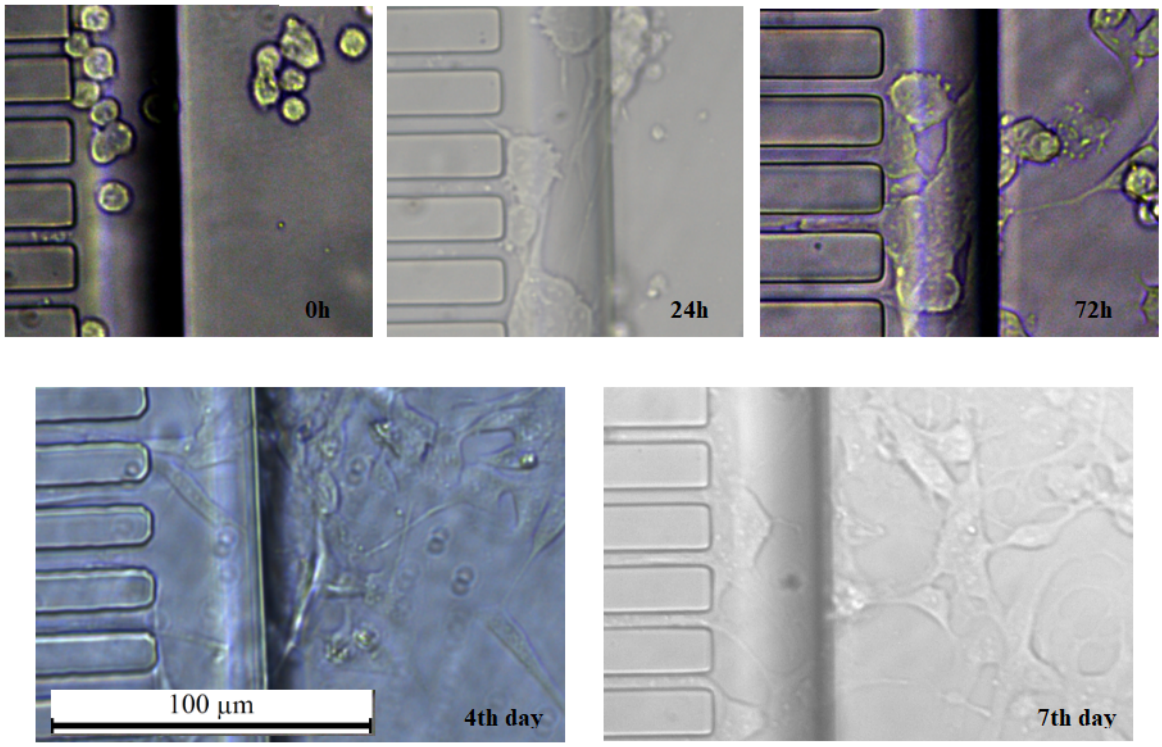

Figure 4.17 Microscope images of SH-SY5Y cell growth in the 7 days. Scale bar: 100 μm.

5. DISCUSSION

The complex structure and physiology of the nervous system have been searched by scientists for years. Scientists have developed different techniques such as compartmentalized systems for investigating the nerve cells which are the functional units of this complex system [6, 10, 14]. Compartmentalized microfluidic chips are one of the systems developed to investigate the function of nerve cells by isolating axons from their cell bodies. Different designs were implemented depending on the purpose of the studies [7, 9, 75].

In this thesis, a microfluidic neuron chip was designed by taking references from previous studies [6, 75] and the manufacturing process was tried to optimize to achieve axon isolation. Different SU-8 photoresist types and UV exposure doses were applied to obtain the ideal microgroove width.

Different microgroove width sizes between 5 μm and 10 μm in different depths were reported in different studies [7, 9, 75]. In one of those studies, [3], axon isolation of SH-SY5Y cells from microgrooves with different height$\times$width sections was evaluated. According to this study, it was observed that microgrooves having 2.5 μm height and 10 μm width weren't efficient for isolating axons and this result was compatible with the results in this thesis. On the other hand, in the same study, it was demonstrated that microgrooves having 2.5$\times$5 μm geometry played a barrier role in preventing the migration of the soma part of the cells. In addition to this, in this thesis, it was observed that microgrooves having larger geometry which is 4$\times$7.7 μm also acted like a barrier for the same cell type and prevented soma migration.

Two different cell culture methods were applied to evaluate the efficiency of the fabricated microfluidic chip. For optimizing an easy and cost-efficient cell seeding method, filtered microfluidic pipette tips were used to seed the cells into the microchannels. Changing the pipette tips during the media change, as well as the applied pressure

and high flow rate caused the detachment of the cells from the channel surface and stay suspended in the liquid. Some of the suspended cells were lost through pipette tips during culture media change. In addition, during the pipette change, the liquid outflow was observed from the channel to the inlet part and this method was not found to be effective since this situation created a risk of contamination. Therefore, this method was not evaluated as an efficient and applicable way of cell seeding in terms of the risk of contamination, cell damage, and bubble formation.

In the second part of the cell culture process, cell seeding through reservoirs with an 8 mm diameter was applied by following the instructions in the study [78] under the Xona Microfluidics Sponsorship. Even though having a similar size of microchannels to the chip in the study, some problems were experienced during the cell loading to the channels in terms of the distance from the microgrooves and cell migration to the reservoir. To eliminate this problem, the cell seeding angle was changed and two-step cell seeding method was tried. Cells were located closer to the microgrooves.

There are many variables affecting the master mold production during SU-8 photolithography since it requires many steps to follow. Soft bake is one of these variables which is required for solvent evaporation and improving the adhesion quality between the substrate and SU-8 layer. Obtaining thicker layers, especially more than 100 μm requires better optimization to be able to have a sufficient amount of residual solvent. While over-baking causes crack formation, under-baking might cause bubble formation and stick to the photomask [79]. Sticking to the mask was one of the problems that occurred during the production of the 2nd layer. To prevent this problem relaxation time was increased up to 15 minutes for both SU-8 3050 and SU-8 2050 coatings. Since SU-8 2050 photoresist is more viscous, the temperature was increased gradually from 65°C to 95°C after the first baking step instead of contacting coated substrate directly with the hot plate at 95°C. These additional steps highly prevented sticking the SU-8 photoresist layer to the photomask.

Variables that were mentioned above such as homogenous SU-8 photoresist coating, baking time, UV exposure dose, and development quality affect the thickness of

patterns on the master molds [42, 79]. Having thicker SU-8 3050 patterns than it was aimed in the second layer of the master mold was associated with nonhomogeneous coating and adding relaxation period after the soft bake process. In addition, some of the variables such as the applied gradual heating method, soft baking and PEB times during SU-8 3005 coating were associated with obtaining different microgroove widths than SU-8 2005 model. Since SU-8 2005 is more viscous and required different baking procedures, this might affect the size of the final structure. These variables were found to be crucial for the reproducibility of the desired results.

Another challenge that is experienced during the production of microfluidic chip fabrication is the adhesion between the PDMS negative templates and the master molds during the peeling-off. Even though PDMS is a flexible material, formed structures on the PDMS negative template and patterns on the master mold might be damaged because of the adhesion. Therefore, the master mold surface was coated with trimethylchlorosilane by the CVD method to eliminate the adhesion problem [76, 77]. This method was used to prevent the PDMS negative mold from lifting off the microgroove patterns during detachment. Using aluminum foil templates during the PDMS curing process and increasing the waiting time at room temperature after the curing step were the other steps added to prevent adhesion.

For future studies, investigating the nerve cells and their interaction with cancer cells can be applied to this microfluidic chip. It has been reported that there is an important interaction between cancer cells and neurons [7]. Some studies suggest that nerve filtration is important to prevent cancer progression, especially prostate cancer progression. Because prostate cancer cells are associated with the overexpression of the precursor of nerve growth factor (proNGF) which triggers axonogenesis. In the literature, Boyden Chamber was used to demonstrate this effect and neurite outgrowth [80]. But there are some disadvantages of this system such as not controlling fluidic separation and axon growth on a porous membrane [10, 4]. To be able to have better axon isolation and observe neurite elongation, multicompartment microfluidic chips are suggested to use. For this purpose, the fabricated microfluidic neuron chip in this thesis study can be used for investigating prostate cancer cell-neuron interaction. SH-SY5Y

cells can be used for observing their reaction against the overexpression of proNGF by prostate cancer cells. The other nerve cell types would also be used by checking their sizes. In addition, this optimized chip can be used with a perfusion control system by opening small inlets. Thus, a dynamic cell culture environment might be created to mimic blood flow and by adding shear stress. In conclusion, cell behaviors might be compared between dynamic and static environments.

6. CONCLUSION

In this thesis study, the effects of different photoresist viscosities, photolithography devices, and UV exposure doses on the microgroove width of microfluidic chips were investigated for neuronal cell culture studies. Ease and repeatability of application and effect of microgroove size on axon isolation were observed by experimenting with two different cell culture methods. During both cell seeding methods, it has been demonstrated that different microgroove widths significantly affect cell migration. Cell migration was observed through the microgrooves with 4.4 μm height and 10.2 μm width while smaller microgroove geometries (4×7.7 μm and 4.4×7.3 μm) played a barrier role and provided axon isolation.

Ideal microgroove geometry (4.4×7.3 μm) was obtained by using SU-8 3005 photoresist coating and 3 seconds of UV exposure time with 21 mW/ cm^2 UV source power. Another master mold with ideal microgroove geometry (4×7.7 μm) was prepared by using the same SU-8 3005 photoresist and different UV lithography system present in the Microfluidic Chip Laboratories of GTU. 4 seconds of UV exposure with 58 mW/cm^2 power was found to be optimum to have the ideal geometry. The main purpose of using this chip was to demonstrate the efficacy of a more economical photolithography device that can be used outside of a cleanroom. And it provided promising results for future studies.

On the other hand, cell seeding through 8 mm wide reservoirs was founded to be a more efficient and replicable cell culture method than the other method. This method was developed and obtained better results by giving an angle to the chips for a short time after cell seeding to make cells contact with microgrooves. Applying a two-step cell seeding method to increase the number of cells by preventing cell migration to the reservoirs was the other modification added to the method. The second cell seeding method with modifications was observed as an optimum method for isolating axons, and carrying out an easy and longer cell culture process without contamination.

In conclusion, the optimized microfluidic chip fabrication and modified cell culture method provided promising results for performing nerve cell culture studies. The fabricated microfluidic chips were evaluated as suitable for future studies to investigate neurite elongation and differentiation of SH-SY5Y cells and their interaction with their microenvironment. Moreover, it is thought that the designed chips can be used in dynamic cell culture studies to mimic in vivo environments by reducing the inlet dimensions.

REFERENCES

1. Silbernagl, S., and A. Despopoulos, *Color Atlas of Physiology. 6th*, Stuttgart: New York: Thieme, 2009.

2. Marani, E., and E. A. Lakke, "Chapter 4 - peripheral nervous system topics," in *The Human Nervous System Third Edition*, pp. 82–140, San Diego: Academic Press, third edition ed., 2012.

3. De Vitis, E., V. La Pesa, F. Gervaso, Romano, and et al., "A microfabricated multi-compartment device for neuron and schwann cell differentiation," *Scientific reports*, Vol. 11, no. 1, pp. 1–12, 2021.

4. Al-Ali, H., S. R. Beckerman, J. L. Bixby, and V. P. Lemmon, "In vitro models of axon regeneration," *Experimental neurology*, Vol. 287, pp. 423–434, 2017.

5. Poliak, S., and E. Peles, "The local differentiation of myelinated axons at nodes of ranvier," *Nature Reviews Neuroscience*, Vol. 4, no. 12, pp. 968–980, 2003.

6. Neto, E., L. Leitão, D. M. Sousa, Alves, and et al., "Compartmentalized microfluidic platforms: the unrivaled breakthrough of in vitro tools for neurobiological research," *Journal of Neuroscience*, Vol. 36, no. 46, pp. 11573–11584, 2016.

7. Lei, Y., J. Li, N. Wang, X. Yang, and et al. Hamada, "An on-chip model for investigating the interaction between neurons and cancer cells," *Integrative Biology*, Vol. 8, no. 3, pp. 359–367, 2016.

8. Kamande, J. W., T. Nagendran, J. Harris, and A. M. Taylor, "Multi-compartment microfluidic device geometry and covalently bound poly-d-lysine influence neuronal maturation," *Frontiers in Bioengineering and Biotechnology*, Vol. 7, p. 84, 2019.

9. Taylor, A. M., M. Blurton-Jones, S. W. Rhee, D. H. Cribbs, and et al., "A microfluidic culture platform for cns axonal injury, regeneration and transport," *Nature methods*, Vol. 2, no. 8, pp. 599–605, 2005.

10. Wang, B., and L. Bao, "Axonal micrornas: localization, function and regulatory mechanism during axon development," *Journal of Molecular Cell Biology*, Vol. 9, no. 2, pp. 82–90, 2017.

11. Vela, F. J., G. Martínez-Chacón, A. Ballestín, J. L. Campos, and et al., "Animal models used to study direct peripheral nerve repair: a systematic review," *Neural regeneration research*, Vol. 15, no. 3, p. 491, 2020.

12. Niculescu, A.-G., C. Chircov, A. C. Bîrcă, and A. M. Grumezescu, "Fabrication and applications of microfluidic devices: A review," *International Journal of Molecular Sciences*, Vol. 22, no. 4, p. 2011, 2021.

13. Cui, P., and S. Wang, "Application of microfluidic chip technology in pharmaceutical analysis: A review," *Journal of pharmaceutical analysis*, Vol. 9, no. 4, pp. 238–247, 2019.

14. Kim, E., and H. Jung, "Local protein synthesis in neuronal axons: why and how we study," *BMB reports*, Vol. 48, no. 3, p. 139, 2015.

15. Campenot, R. B., "Local control of neurite development by nerve growth factor," *Proceedings of the National Academy of Sciences*, Vol. 74, no. 10, pp. 4516–4519, 1977.

16. Boyden, S., "The chemotactic effect of mixtures of antibody and antigen on polymorphonuclear leucocytes," *The Journal of experimental medicine*, Vol. 115, no. 3, pp. 453–466, 1962.

17. Brunello, C. A., V. Jokinen, P. Sakha, Terazono, and et al., "Microtechnologies to fuel neurobiological research with nanometer precision," *Journal of nanobiotechnology*, Vol. 11, no. 1, pp. 1–8, 2013.

18. Rhee, S. W., A. M. Taylor, C. H. Tu, D. H. Cribbs, and et al., "Patterned cell culture inside microfluidic devices," *Lab on a Chip*, Vol. 5, no. 1, pp. 102–107, 2005.

19. Fiorini, G. S., and D. T. Chiu, "Disposable microfluidic devices: fabrication, function, and application," *BioTechniques*, Vol. 38, no. 3, pp. 429–446, 2005.

20. Gale, B. K., A. R. Jafek, C. J. Lambert, B. L. Goenner, and et al., "A review of current methods in microfluidic device fabrication and future commercialization prospects," *Inventions*, Vol. 3, no. 3, p. 60, 2018.

21. Park, J., H. Koito, J. Li, and A. Han, "Multi-compartment neuron–glia co-culture platform for localized cns axon–glia interaction study," *Lab on a Chip*, Vol. 12, no. 18, pp. 3296–3304, 2012.

22. Schmidt, C. E., and J. B. Leach, "Neural tissue engineering: strategies for repair and regeneration," *Annual review of biomedical engineering*, Vol. 5, no. 1, pp. 293–347, 2003.

23. Doblado, L. R., C. Martínez-Ramos, and M. M. Pradas, "Biomaterials for neural tissue engineering," *Frontiers in Nanotechnology*, Vol. 3, p. 643507, 2021.

24. Siddique, R., and N. Thakor, "Investigation of nerve injury through microfluidic devices," *Journal of The Royal Society Interface*, Vol. 11, no. 90, p. 20130676, 2014.

25. Millet, L. J., and M. U. Gillette, "Over a century of neuron culture: from the hanging drop to microfluidic devices," *The Yale journal of biology and medicine*, Vol. 85, no. 4, p. 501, 2012.

26. Park, J., H. Koito, J. Li, and A. Han, "Microfluidic compartmentalized co-culture platform for cns axon myelination research," *Biomedical microdevices*, Vol. 11, no. 6, pp. 1145–1153, 2009.

27. Jocher, G., S. H. Mannschatz, M. Offterdinger, and R. Schweigreiter, "Microfluidics of small-population neurons allows for a precise quantification of the peripheral axonal growth state," *Frontiers in cellular neuroscience*, Vol. 12, p. 166, 2018.

28. Di Paolo, A., J. Garat, G. Eastman, J. Farias, and et al., "Functional genomics of axons and synapses to understand neurodegenerative diseases," *Frontiers in Cellular Neuroscience*, p. 240, 2021.

29. Taylor, A. M., S. W. Rhee, C. H. Tu, D. H. Cribbs, and et al., "Microfluidic multicompartment device for neuroscience research," *Langmuir*, Vol. 19, no. 5, pp. 1551–1556, 2003.

30. Gupta, P., A. Shinde, K. Illath, S. Kar, and et al., "Microfluidic platforms for single neuron analysis," *Materials Today Bio*, p. 100222, 2022.

31. Coquinco, A., L. Kojic, W. Wen, Y. T. Wang, and et al., "A microfluidic based in vitro model of synaptic competition," *Molecular and Cellular Neuroscience*, Vol. 60, pp. 43–52, 2014.

32. Mack, C., *Fundamental principles of optical lithography: the science of microfabrication*, Vest Sussex: John Wiley & Sons, 2007.

33. Gritsch, L., D. Meng, and A. Boccaccini, "20 - nanostructured biocomposites for tissue engineering scaffolds," in *Biomedical Composites (Second Edition)*, pp. 501–542, Woodhead Publishing, 2017.

34. Cha, C., F. Piraino, and A. Khademhosseini, "Chapter 9 - microfabrication technology in tissue engineering," in *Tissue Engineering (Second Edition)*, pp. 283–310, Oxford: Academic Press, second edition ed., 2014.

35. Venkatakrishnan, K., B. Ngoi, P. Stanley, L. Lim, and et al., "Laser writing techniques for photomask fabrication using a femtosecond laser," *Applied Physics A*, Vol. 74, no. 4, pp. 493–496, 2002.

36. Li, C.-W., and G.-J. Wang, "8 - mems manufacturing techniques for tissue scaffolding devices," in *MEMS for Biomedical Applications*, pp. 192–217, Woodhead Publishing, 2012.

37. Singh, J. P., R. Bhardwaj, A. Sharma, B. Kaur, and et al., "Chapter 2 - fabrication of magnetic tunnel junctions," in *Advanced Applications in Manufacturing Enginering*, pp. 53–77, Woodhead Publishing, 2019.

38. Scott, S. M., and Z. Ali, "Fabrication methods for microfluidic devices: An overview," *Micromachines*, Vol. 12, no. 3, p. 319, 2021.

39. Quero, J. M., F. Perdigones, and C. Aracil, "11 - microfabrication technologies used for creating smart devices for industrial applications," in *Smart Sensors and MEMs (Second Edition)*, pp. 291–311, Woodhead Publishing, second edition ed., 2018.

40. Hennessy, T. C., *Lithography: principles, processes and materials*, Nova Science,.

41. Ren, K., J. Zhou, and H. Wu, "Materials for microfluidic chip fabrication," *Accounts of chemical research*, Vol. 46, no. 11, pp. 2396–2406, 2013.

42. Mata, A., A. J. Fleischman, and S. Roy, "Fabrication of multi-layer su-8 microstructures," *Journal of micromechanics and microengineering*, Vol. 16, no. 2, p. 276, 2006.

43. Chang, H.-K., and Y.-K. Kim, "Uv-liga process for high aspect ratio structure using stress barrier and c-shaped etch hole," *Sensors and Actuators A: Physical*, Vol. 84, no. 3, pp. 342–350, 2000.

44. Zhang, J., M. B. Chan-Park, and S. R. Conner, "Effect of exposure dose on the replication fidelity and profile of very high aspect ratio microchannels in su-8," *Lab on a Chip*, Vol. 4, no. 6, pp. 646–653, 2004.

45. Lorenz, H., M. Despont, N. Fahrni, J. Brugger, and et al., "High-aspect-ratio, ultrathick, negative-tone near-uv photoresist and its applications for mems," *Sensors and Actuators A: physical*, Vol. 64, no. 1, pp. 33–39, 1998.

46. Gale, B. K., A. R. Jafek, C. J. Lambert, B. L. Goenner, and et al., "A review of current methods in microfluidic device fabrication and future commercialization prospects," *Inventions*, Vol. 3, no. 3, p. 60, 2018.

47. Miranda, I., A. Souza, P. Sousa, J. Ribeiro, and et al., "Properties and applications of pdms for biomedical engineering: A review," *Journal of Functional Biomaterials*, Vol. 13, no. 1, p. 2, 2021.

48. Victor, A., J. Ribeiro, and F. F. Araújo, "Study of pdms characterization and its applications in biomedicine: A review," *Journal of Mechanical Engineering and Biomechanics*, Vol. 4, no. 1, pp. 1–9, 2019.

49. Rodrigues, R. O., D. Pinho, D. Bento, R. Lima, and et al., "Wall expansion assessment of an intracranial aneurysm model by a 3d digital image correlation system," *Measurement*, Vol. 88, pp. 262–270, 2016.

50. Kuncová-Kallio, J., and P. J. Kallio, "Pdms and its suitability for analytical microfluidic devices," in *2006 International Conference of the IEEE Engineering in Medicine and Biology Society*, pp. 2486–2489, IEEE, 2006.

51. Hemmilä, S., J. V. Cauich-Rodríguez, J. Kreutzer, and P. Kallio, "Rapid, simple, and cost-effective treatments to achieve long-term hydrophilic pdms surfaces," *Applied Surface Science*, Vol. 258, no. 24, pp. 9864–9875, 2012.

52. Zhao, J., D. A. Sheadel, and W. Xue, "Surface treatment of polymers for the fabrication of all-polymer mems devices," *Sensors and Actuators A: Physical*, Vol. 187, pp. 43–49, 2012.

53. Rivet, C., H. Lee, A. Hirsch, S. Hamilton, and et al., "Microfluidics for medical diagnostics and biosensors," *Chemical Engineering Science*, Vol. 66, no. 7, pp. 1490–1507, 2011.

54. Ren, K., J. Zhou, and H. Wu, "Materials for microfluidic chip fabrication," *Accounts of chemical research*, Vol. 46, no. 11, pp. 2396–2406, 2013.

55. Nielsen, J. B., R. L. Hanson, H. M. Almughamsi, C. Pang, and et al., "Microfluidics: Innovations in materials and their fabrication and functionalization," *Analytical chemistry*, Vol. 92, no. 1, pp. 150–168, 2019.

56. Vlachopoulou, M.-E., P. Petrou, S. Kakabakos, A. Tserepi, and et al., "Effect of surface nanostructuring of pdms on wetting properties, hydrophobic recovery and protein adsorption," *Microelectronic Engineering*, Vol. 86, no. 4-6, pp. 1321–1324, 2009.

57. Lee, J. N., C. Park, and G. M. Whitesides, "Solvent compatibility of poly (dimethylsiloxane)-based microfluidic devices," *Analytical chemistry*, Vol. 75, no. 23, pp. 6544–6554, 2003.

58. Akther, F., S. B. Yakob, N.-T. Nguyen, and H. T. Ta, "Surface modification techniques for endothelial cell seeding in pdms microfluidic devices," *Biosensors*, Vol. 10, no. 11, p. 182, 2020.

59. Belkind, A., and S. Gershman, "Plasma cleaning of surfaces," *Vacuum Coating and Technology November*, pp. 46–57, 2008.

60. Borók, A., K. Laboda, and A. Bonyár, "Pdms bonding technologies for microfluidic applications: A review," *Biosensors*, Vol. 11, no. 8, p. 292, 2021.

61. Miranda, I., A. Souza, P. Sousa, J. Ribeiro, and et al., "Properties and applications of pdms for biomedical engineering: A review," *Journal of Functional Biomaterials*, Vol. 13, no. 1, p. 2, 2021.

62. Hassanpour-Tamrin, S., A. Sanati-Nezhad, and A. Sen, "A simple and low-cost approach for irreversible bonding of polymethylmethacrylate and polydimethylsiloxane at room temperature for high-pressure hybrid microfluidics," *Scientific Reports*, Vol. 11, no. 1, pp. 1–12, 2021.

63. Becker, H., and U. Heim, "Hot embossing as a method for the fabrication of polymer high aspect ratio structures," *Sensors and Actuators A: Physical*, Vol. 83, no. 1-3, pp. 130–135, 2000.

64. Becker, H., and L. E. Locascio, "Polymer microfluidic devices," *Talanta*, Vol. 56, no. 2, pp. 267–287, 2002.

65. Ng, S., Z. Wang, R. Tjeung, and N. F. de Rooij, "Development of a multi-layer microelectrofluidic platform," *Microsystem technologies*, Vol. 13, no. 11, pp. 1509–1515, 2007.

66. McCormick, R. M., R. J. Nelson, M. G. Alonso-Amigo, D. J. Benvegnu, and et al., "Microchannel electrophoretic separations of dna in injection-molded plastic substrates," *Analytical Chemistry*, Vol. 69, no. 14, pp. 2626–2630, 1997.

67. Attia, U. M., S. Marson, and J. R. Alcock, "Micro-injection moulding of polymer microfluidic devices," *Microfluidics and nanofluidics*, Vol. 7, no. 1, pp. 1–28, 2009.

68. Giboz, J., T. Copponnex, and P. Mélé, "Microinjection molding of thermoplastic polymers: a review," *Journal of micromechanics and microengineering*, Vol. 17, no. 6, p. R96, 2007.

69. Hwang, J., Y. H. Cho, M. S. Park, and B. H. Kim, "Microchannel fabrication on glass materials for microfluidic devices," *International Journal of Precision Engineering and Manufacturing*, Vol. 20, no. 3, pp. 479–495, 2019.

70. Kotz, F., M. Mader, N. Dellen, P. Risch, and et al., "Fused deposition modeling of microfluidic chips in polymethylmethacrylate," *Micromachines*, Vol. 11, no. 9, p. 873, 2020.

71. Sharafeldin, M., A. Jones, and J. F. Rusling, "3d-printed biosensor arrays for medical diagnostics," *Micromachines*, Vol. 9, no. 8, p. 394, 2018.

72. Mohamed, O. A., S. H. Masood, and J. L. Bhowmik, "Optimization of fused deposition modeling process parameters: a review of current research and future prospects," *Advances in manufacturing*, Vol. 3, no. 1, pp. 42–53, 2015.

73. Wang, X., M. Jiang, Z. Zhou, J. Gou, and et al., "3d printing of polymer matrix composites: A review and prospective," *Composites Part B: Engineering*, Vol. 110, pp. 442–458, 2017.

74. Van den Driesche, S., F. Lucklum, F. Bunge, and M. J. Vellekoop, "3d printing solutions for microfluidic chip-to-world connections," *Micromachines*, Vol. 9, no. 2, p. 71, 2018.

75. Harris, J., H. Lee, B. Vahidi, C. Tu, and et al., "Fabrication of a microfluidic device for the compartmentalization of neuron soma and axons," *JoVE (Journal of Visualized Experiments)*, no. 7, p. e261, 2007.

76. Liu, J., D. Zhang, B. Sha, P. Yin, and et al., "Fabrication of a three-layer su-8 mould with inverted t-shaped cavities based on a sacrificial photoresist layer technique," *Biomedical microdevices*, Vol. 16, no. 5, pp. 655–660, 2014.

77. Tümer, E. H., H. Y. Erbil, and N. Akdoğan, "Wetting of superhydrophobic polylactic acid micropillared patterns," *Langmuir*, 2022.

78. Nagendran, T., V. Poole, J. Harris, and A. M. Taylor, "Use of pre-assembled plastic microfluidic chips for compartmentalizing primary murine neurons," *JoVE (Journal of Visualized Experiments)*, no. 141, p. e58421, 2018.

79. Martinez-Duarte, R., and M. Madou, *SU-8 Photolithography and Its Impact on Microfluidics*, pp. 231–268. 09 2010.

80. Pundavela, J., Y. Demont, P. Jobling, L. F. Lincz, S. Roselli, R. F. Thorne, D. Bond, R. A. Bradshaw, M. M. Walker, and H. Hondermarck, "Prongf correlates with gleason score and is a potential driver of nerve infiltration in prostate cancer," *The American journal of pathology*, Vol. 184, no. 12, pp. 3156–3162, 2014.